NTNU – Trondheim
Norwegian University of
Science and Technology

Short simulation approach for floating offshore wind turbine design load case

Ekrem Tiyip

Supervisor
Prof.Jørgen Amdahl
Co-Supervisor
PhD-candidate Stian Sørum

NTNU, 2020
Faculty of Engineering and Science
Department of Marine Technology

Abstract

Comparing the results of various simulation approaches in SIMA on a critical ultimate limit state (ULS) design driver, the present project work aims to purpose a short-simulation approach to save computational time for the design process of the floating offshore wind turbines (FOWT).
The design process of an FOWT is a complex task because of the coupling between the aerodynamics, hydrodynamics, structural dynamics and the behavior of the controller. The nonlinear time domain simulation is recommended to analyze the coupled structural responses. To ensure the structural integrity and safety, the design rules specified a minimum set of combination of the external conditions and the design situations. The full set-up ends up 100 to 10000 load cases and becomes computationally demanded. Therefor, focusing on the critical load cases in the early stages of design is a common practice. A proper assessment on the combinations of the environmental parameters and the properties of the concept can reduce the load case set-up significantly.
The long natural period of the floaters requires longer simulation time in the load cases where the wave loads are important. Namely, minimum one-hour simulation length is recommended in DLCs using extreme sea state/severe sea state. Further, during the conceptional and initial sizing phase, designer needs to update the structural parameters constantly to get the optimal design. Repeating the one-hour simulations with several seeds many times are time consuming. Therefore, an alternative simulation approach is in interest.
If the coupled structural response at the extreme waves sufficiently describes the maximum response of the full simulation, then a few seconds short-simulation with proper initialization can be used for the characteristic value estimation.
Current study investigates the applicability of the short-simulation approach to estimate a characteristic value for ULS in a specific design driver. The tower base bending moment in DLC_6.1 is in focus, the coupled time domain aero-hydro-servo-elastic analysis carried on a numerical model in SIMA. The numerical model is a 10MW wind turbine supported by a spar buoy. The results of the short-simulation approach compared with the characteristic responses estimated by full one-hour simulations.
Keywords: Floating offshore wind turbines (FOWT); Reducing simiulation time; short-simulation approach; Design load case (DLC); Spar ; Nonlinear time domain simulation; SIMA

Acknowledgements

This work was the master thesis in the spring semester in 2020. Specifically, aimed for a short-simulation approach to save computational time for the design process of the FOWT. I would like to thank the following people for their support, without whose help this work would never have been possible:
Supervisor Professor Jørgen Amdahl and co-supervisor PhD candidate Stian Sørum.

Ekrem Tiyip
10.06.2020 Drammen

NTNU
Norges teknisk-naturvitenskapelige universitet
Institutt for marin teknikk

MASTER THESIS 2020

for

Stud. techn. Ekrem Tiyip

Design load cases for offshore wind turbines

Designlaster for offshore vindturbiner

Background:
In order to obtain class approval of an offshore wind turbine, thousands of design load cases (DLCs) need to be considered. These DLCs include a wide range of operational, parked, and fault conditions, and are used to ensure that the structure has sufficient strength to withstand both fatigue and extreme loads over its design lifetime.

The extensive DLCs suggested by the standards require significant computational effort during design. In some cases, the DLCs may be difficult to interpret, or different modelling approaches may give significantly different result. It is therefore of interest to identify design-driving load cases – and to determine how some of the deterministic load cases compare to stochastic simulations with irregular waves and turbulent wind.

During the thesis work in the spring, a more thorough comparison of the deterministic and stochastic load cases is anticipated. In the fall, the main focus will be on becoming familiar with the design standards and with the dynamics of offshore wind turbines.

The following topics should be addressed in the project work:

1. Describe the dynamics of different support structures on a general level and on this basis motivate why a SPAR buoy is selected. Provide a detailed description of the SPAR buoy including tower and the 10 MW wind turbine and how it is modelled for time domain analysis in SIMA. Describe the environmental conditions at the selected site. Discuss which load cases that may be most relevant with respect to fatigue and ultimate strength criteria and how these loads can be simulated in SIMA.

2. Project work revisited. Simulations carried out for a period of 1 hour are considered to give the reference values for the ultimate strength of key response parameters. For each 1-hour period identify the wave height order associated with the maximum response within a certain period range. For these cases repeat simulation for a limited time period of the maximum response and record the maximum response for the short simulation. Identity the period length and temporal location that is required to obtain sufficient decay of the transient response. Compare the extreme value distributions for the two approaches.

3. Repeat the above simulations for a number of environmental conditions with different wave height and periods to verify the selected approach. If necessary, suggest simple correction factors etc. that may be adopted to get more accurate results.

4. Investigate if the adopted procedure is valid also when turbulent wind is considered, and when the wind and waves are misaligned.

5. Conclusions and recommendations for further work

Literature studies of specific topics relevant to the thesis work may be included.

The work scope may prove to be larger than initially anticipated. Subject to approval from the supervisors, topics may be deleted from the list above or reduced in extent.

In the thesis the candidate shall present his personal contribution to the resolution of problems within the scope of the thesis work.

Theories and conclusions should be based on mathematical derivations and/or logic reasoning identifying the various steps in the deduction.

The candidate should utilise the existing possibilities for obtaining relevant literature.

Thesis format
The thesis should be organised in a rational manner to give a clear exposition of results, assessments, and conclusions. The text should be brief and to the point, with a clear language. Telegraphic language should be avoided.

The thesis shall contain the following elements: A text defining the scope, preface, list of contents, summary, main body of thesis, conclusions with recommendations for further work, list of symbols and acronyms, references and (optional) appendices. All figures, tables and equations shall be numerated.

The supervisors may require that the candidate, in an early stage of the work, presents a written plan for the completion of the work. The plan should include a budget for the use of computer and laboratory resources which will be charged to the department. Overruns shall be reported to the supervisors.

The original contribution of the candidate and material taken from other sources shall be clearly defined. Work from other sources shall be properly referenced using an acknowledged referencing system.

The report shall be submitted electronically in pdf format:
- Signed by the candidate
- The text defining the scope included
- Drawings and/or computer prints which cannot be bound should be organised in a separate folder.
- Essential input files for computer analysis, spreadsheets, Matlab files etc submitted in digital format

Supervisor:
Prof. Jørgen Amdahl

Co-supervisor:
PhD-candidate Stian Sørum

Deadline: June 10, 2020

Trondheim, January 15, 2020

Jørgen Amdahl
Professor

Contents

List of Figures

List Of Abbrivations

ALS	Accidental Limit State
BEM	Blade Element Momentum Theory
DOF	Degree of Freedom
DLC	Design Load Case
ESS	Extreme Sea State
EWM	Extreme Wind speed Model
ECM	Extreme Current Model
EWLR	Extreme Water Level Range
FOWT	Floating Offshore Wind Turbine
FLS	Fatigue Limit State
TLP	Tension Leg Platform
NEK	Norsk Elektroteknisk Komite
NSS	Normal Sea State
NKUA	National Kapodistrian Uni-versity of Athens
OWT	Offshore Wind Turbine
RNA	Rotor Nacelle Assembly
ULS	Ultimate Limit State
SLS	Serviceability Limit State
SSS	Severe Sea State
VIV	Vortex-Induced Vibration

Chapter 1

Introduction

The offshore wind energy is attracting interest because of the environmental issues caused by burning fossil fuels. The EU planned to reduce the CO_2 emission to 15-20% of the 1990s level by 2050. On the contrary, the demand on energy is expected to increasing in a while. Therefore, the further development in renewable energy is a key to achieve the environmental goal. The offshore wind energy is one of the renewable energy source that available in Europe [1].

Installing wind turbines on offshore have several advantages such as large available area, convenience in transportation, higher wind speed and less turbulence. Even so, it is still poorly profitable in transient and deep water for expenses in installation, maintenance and computationally demanded design process. Shallow waters with high wind energy density are limited; the industry needs further development in transient and deep water. Supporting wind turbines with floater is an alternative solution in transient water, while it is the only way to go in deep water.
Standards defined the combination of design situations and external conditions as load cases. Further more, they required a minimum set of load cases to analyze for ensuring the structural integrity and safety. The full set-up load case list ends up with a 100-10000 load case which should be properly considered in the final stage of the design process. A reduced number of load case set-up can be used during the conceptional design process. The critical load cases for a specific concept can determine by carefully analyzing the variations and combinations of environmental load.
Designing process of FOWT is computationally demanded. Because of the floater structures have a lengthy natural period, to capturing the slowly varying responses one needs to simulate longer; usually 1-hour simulation length is applied. Further more, some simplified approaches that used in bottom fixed structures are not applicable. For example, the embedded wave approach is not suitable when natural periods are longer than wave periods [3].Running the coupled time domain simulation after each change is time consuming.
The current study aims to reducing the simulation time in FOWT design process. Specifically, the investigation focused on the extreme response prediction in the extreme environmental condition which has a 50 years return period. In the storm conditions where the wind speed above the cut-off speed, normally the turbine is parked to prevent structural damage; the corresponding design load case in standard is DLC_6.1 [6].
In the DNVGL-ST-0119, the USL control for design of FOWT structures defined as the 98% quantile in the distribution of the annual maximum combined load effect [4]. It is the combined load effect that has a 50 years return period. The proper way of estimating characteristic response is to carrying a stochastic long-term response analysis which is an enormous work. The standards allow to estimating the characteristic response as the expected value of the short-term extreme response distribution in the worst environmental state which has a 50 years return period. The characteristic design value than estimated as a mean value of five simulations maximums [4].
The five-hour simulation is an enormous improvement compare to a full long-term response analysis. However, as mentioned, the simulation length should be long enough to capture the nonlinearity in the motion when the subject is a floating structure. Repeating the characteristic response estimation again and again after each change is time consuming. The inconvenience is significant for design optimization. In modern computers,we can generate the surface elevations in a quick time.

Thus, the time domain simulation uses the main computational effort for the dynamic calculations in time steps. If it is possible to identify when the maximum response happens, then one need to carry the dynamic calculation in a quick time interval. In this study, we assumed to the occurrence of maximum response related to the maximums of wave time series. In other words, few short simulations at wave maximums may give a sufficient full simulation result.
The Norsk Elektroteknisk Komite (NEK) published the design rules IEC 61400-3-2 for floating support structures of the wind turbine, and the last update is in 2019 [11]. The DNVGL-ST-0119 works for the same purpose; the latest version is in 2018. The requirements are almost identical. In this study, we are applying the requirements from DNVGL. For load calculation, the requirements from DNVGL-ST-0437 is applied. About the practical problems related coupled analysis of wind turbine the DNVGL-RP-126 is used.
The model in the study is a DTU-10MW wind turbine witch supported on a spar-buoy floating support structure. We chose the site and pick the corresponding extreme environmental condition parameters from [10].
In the first phase of the study, 100 one-hour simulation carried on the simplified DLC_6.1 to have a reference extreme value distribution. Further investigations carried for understanding when the maximum responses shows up. Based on the results, we came up with suggestions to short simulation approaches that may work for characteristic response estimation.
The second phase is investigating the minimum reasonable time for initialization. The initialization period is the used time for the dynamic equilibrium in dynamic calculation. It depends on the applied software and the controller algorithm. The initialization period is also longer for floating structures than fixed ones. The recommendation is minimum 600 seconds [5]. However, it can be shorter in our case where the blade pitch angel set to be zero in advance.
In the last phase, the results of the short simulation approaches compared with the full simulation generated characteristic responses.
The project report is structured as follows:

- The Chapter 2 summarizes the existing concepts, important statements of the design rules and the critical load cases for FOWT.

- The Chapter 3 is the brief presentation of the current study related theories.

- The Chapter 4 gives a brief introduction to the numerical model.

- The chapter 5, 6, 7 presents the method and the result of the current project in three phases.

- The chapter 8 is discussion, conclusion and recommendation for further work.

Chapter 2

Floating offshore wind turbines

2.1 Common bottom fixed structures

The common bottom fixed support structures are not ideal for deeper waters. The simple and cost effective concept of the offshore wind turbine support structure is monopile. The monopile concept is easier to manufacturing and installing witch makes the monopile the most used OWT support structure. The natural periods are small and the coupling effects can be neglected. However, it is a concept for smaller wind turbines in shallow water. In recent years, the interest expanding to transient and deep water areas, and the turbine sizes are exploding for the optimal effect to the investment. As a result, further development of monopiles facing additional challenges. For instance, the resistance of the soil and the hydrodynamic behavior of a large diameter pile are the limiting factors. The feasibility of the concept to deeper waters and larger turbines is further discussed in [14].
The jacket structure is an alterative OWT support structure for water depth of 30m to 90m. The jackets are applied in oil and gas industry for decays. Thus, there are available engineering knowledge from design process to installation. The natural periods are small and we can neglect the coupling between wind and wave in some designs. However, the jacket is not economically workable for OWT in deep water.The application of jacket structure further discussed in [15].

2.2 Common floater concepts

The future of OWT industry needs more development in FOWT. Particularly, cost efficient and reliable floater design is the solution for expanding offshore wind energy production to deep water. Stability of the floaters: The roll and pitch restoring moments expressed as:

$$M_{R,roll} = [(\rho g I_{xx}) + (F_B Z_{CB} - mgZ_{CG}) + (C_{44,moor})]sin(\phi) \tag{2.1}$$

$$M_{R,roll} = [(\rho g I_{yy}) + (F_B Z_{CB} - mgZ_{CG}) + (C_{55,moor})]sin(\theta) \tag{2.2}$$

The static stability of the floater in roll and pitch can be achieved in unique ways [2]. Based on witch term in the Equation (2.1) and Equation (2.2) dominates, the concepts are classified as buoyancy stabilized, ballast stabilized and mooring line stabilized floaters.
The spar concept is a ballast stabilized floater with a long draft. To lowering the center of gravity, the bottom part of the structure filled with water or concrete. It is simple in design, easy to install. However, the long draft limits its applicability to deep water. Not suitable for transient water. The first full scale floating wind turbine was Equinor's hywind concept and constructed in 2010 in Norway. The support structure of Hywind concept is a huge spar buoy.
The natural period in heave generally larger than 25 second and the heave motion is slight because of a long draft. The current loads and the vortex-induced oscillation can be important. The coupling between yaw and pitch motion should be avoided because of low yaw stiffness. The coupling between heave and pitch can also occur and cause instability [4].
Semi-Submersibles is a buoyancy/ballast stabilized floater. The concept suitable for shellow water

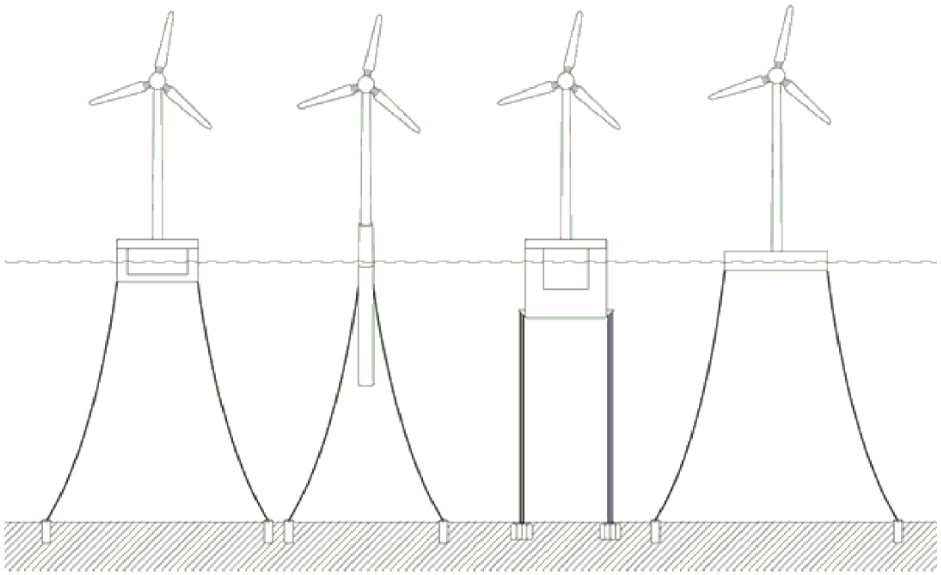

Figure 2.1: The types of floating support structures for wind turbines [4]

to transient water because of shellow draft. The shapes of the support columns can be in various shapes. The heave natural period can be exited under extreme wave condition [4]
Tension Leg Platform (TLP): The TLP support structures is a mooring line stabilized floater and keeps the static stability with high pretensions in the mooring lines. The natural frequencies in heave and pitch is smaller than wave frequencies. The sum frequency can cause springing and ringing responses and important for the fatigue of tethers[4] Because of the high installation cost, it is not a popular floating wind turbine concept. [2].
The boundary condition for the concepts are presented in Table 2.1; the general natural period ranges are presented in Table 2.2.

Concepts	Surge	Sway	Heave	Roll	Pitch	Yaw
Spar	C	C	C	C	C	C
Semi-Submersible	C	C	C	C	C	C
Barge	C	C	C	C	C	C
Tension leg platform (TPL)	C	C	C	R	R	C

C = compaliant
R = restrained

Table 2.1: The boundary conditions of the common FOWT concepts [4]

Concepts	Surge	Heave	Pitch	Yaw
Spar	≈ 100	25-40	25-40	5-20
Semi-Submersible	≈ 100	15-25	25-40	50-80
Barge	≈ 100	5-10	9-16	50-100
Tension leg platform (TPL)	15-60	1-2	2-5	8-20

units = [s]

Table 2.2: Natural period of common floaters [3]

2.3 Design principles

The design principles and requirements for support structures and their stations keeping system is provided in DNVGL-ST-0119[4]. The offshore wind turbine is unmanned in most of the time. The service and maintaining process is requiring man power, but usually it carries under the good

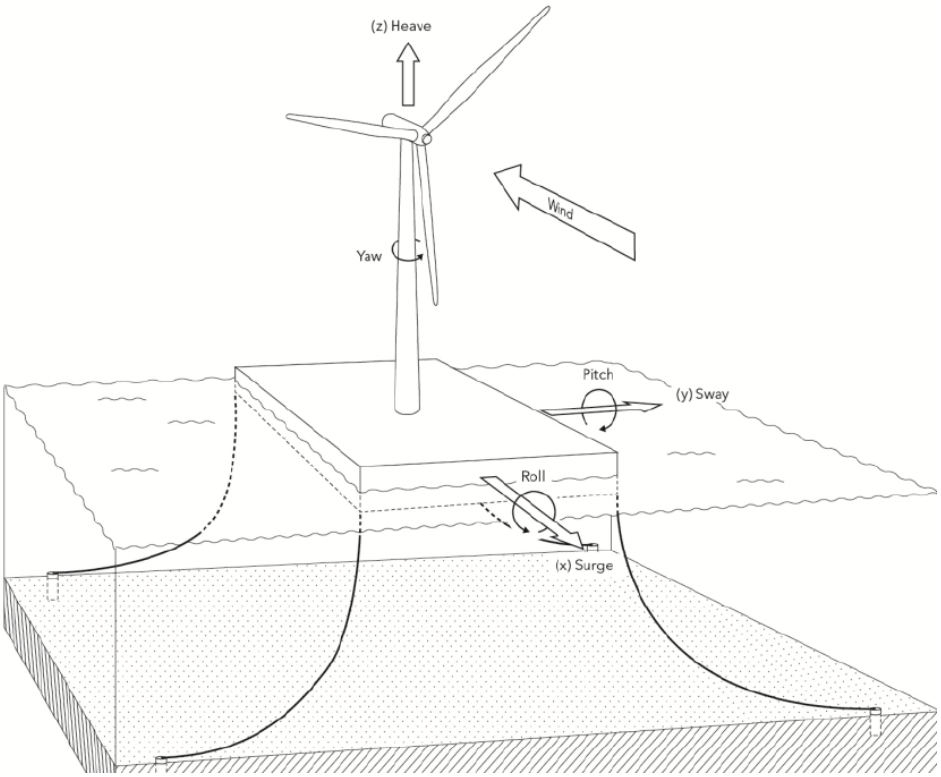

Figure 2.2: 6 DOFs of wind turbine [4]

Surge: Displacement along the longitudinal axis
Sway: Displacement along the lateral axis
Heave: Displacement along the vertical axis
Roll: Rotation about the longitudinal axis
Pitch: Rotation about the lateral axis
Yaw: Rotation about the vertical axis

weather condition. In addition, the offshore wind turbines are located an interminable distance away from shore, and there should stand along. Therefore, the failure has a negligible possibility to create serious consequences and the major loss has an economical nature. Hence, normally OWT structure and its station keeping system design to consequence class 1 which loss of structure is acceptable.
The design rules specified several limit states for the structure to be qualified, such as ultimate limit state (ULS), fatigue limit state (FLS), accidental limit state (ALS) and serviceability limit state (SLS).
The ULS covers the yielding, buckling, brittle fracture, stability and critical deformations.
The FLS covers the cumulative damage because of repeated load cycles.
The ALS covers the global and local damage by accidents and the damage caused resistance reduction.
Serviceability limit state (SLS) covers the displacements, deformations, vibrations and failure in individual component failures that can disturb the normal production of OWT. In this study the focus is on ULS. Because of the nonlinearity of the dynamics in FOWT, the direct time domain simulation of the combined load effect is perfered. The DNVGL standard allows to use the design by partial safety factor method together with simulation. The design inequality defined as the design load effect should be smaller than the structural resistance.

$$S_d \leq R_d \tag{2.3}$$

The design load effect S_d defined as the characteristic load effect S_K times a load factor γ_f.

$$S_d = \gamma_f S_K \tag{2.4}$$

The design resistance R_d defined as the characteristic resistance R_K times a material factor γ_m.

$$R_d = \frac{1}{\gamma_m} R_K \tag{2.5}$$

When carrying the ULS analysis, the characteristic load effect S_k is the annual maximum combined load effect that has 50 years return period. The characteristic resistance R_k defined as the 5% quantile in the structural resistance distribution. The $gamma_m$ is the material factor. The specified load factor γ_f is including the variations of the loads from expected value and uncertainties associated with models and the methods of determining characteristic load effect. The values of the load factor for ULS specified in the DNVGL-ST-019 as following .

Load factor set*	G	Q	E**	D	P
ULS (a)	1.25	1.25	0.7	1.0	0.9/1.1
ULS (b)	1.0	1	1.35	1.0	0.9/1.1

G = Permenent load
Q = variable functional load
E = Environmental load
D = Deformation load
P = Prestressing
** The ULS (a) applied for the cases where the permanent load or variable functional load is dominating, such as pretension, lifting forces and static pressure. The ULS (b) applied, on the other hand, in case the environmental load is dominating.*
*** Environmental loads to consequence class 1*

Table 2.3: Parial safety factor γ_f for ULS [6]

2.4 The load cases of FOWT

The current section of the report written closely following the Recommended Practice for Coupled Analysis of Floating Wind Turbines [3].
A full set-up of load cases can be 100 to 10000 in an FOWT, which is required in the last stage of the design process. The analysis should be carried with a proper simulation length and sufficient number of seeds. However, a reduced number of load case set-up can be used during the early phase of the design process. The critical load cases which should be analyzed can determined by a proper assessment of variations and combinations of environmental loads without loosing reliability of the design. Therefor determining the design driving loads are important.
There are several approaches for decide the reduced number of load case set-up. The commonly used one are the sensitivity study, brute force method, experience from a previous project and reduced simulation models.

2.4.1 Ultimate limit state (ULS)

The ULS loads most probability occurs at the extreme environmental state which has a 50 years return period. The unfavorable misalignment can generate extreme loads as well. The failure in controller, failure in brake system, leakage in the floater and mooring line damage can also drive extreme loads. The most relevant DLCs for ULS:
DLC 1.3: The major load components on the RNA can be critical.
DLC 1.4: The load components on the RNA can be critical, specially the yaw bearing overturning moments, hub out-of-plane moments and blade flatwise loads.
DLC 1.6: The extreme hub trust force can occur because of the severe sea state combines with large pitch angle. The largest mean line tension can occur around rated speed due to the combined effect of current and aerodynamic trust.
DLC 6.1: The torque about the rotor axis is critical because of storm wind speed and feathered blades.
The large global motions can results an enormous force in Nacell structure.

The tower base banding moment is critical in this load case because of the combination of large wave loads and wind loads. In addition, the extreme current contribute with healing angle to add extra tower base banding moment. On a spar structure which is long drafted, the effect of current can be significant to tower base banding moment. Espectially, when the wind and current acts from opposite direction.
A large dynamic mooring line tension can be present in this load case as well.
DLC 6.2: Enormous blade torsional loads can occur because of storm wind speed and a large angle of attack.
Because of the unfunctional ballast system, the leakage during a storm can add extra gravitational loads to the tower base.
The critical points specific to a spar concept: The long draft makes relative directions between wave and current important.
Low yaw misalignment makes the turbulence and misalignment specially important.

Floating structures requires longer simulation because of longer natural periods. The 10 minutes simulations not adequate to capture nonlinearity in FOWT. 10 minutes simulation can be applied if the loads dominated by the wind loads. In case where the wave loads are dominated minimum 3 hour should be applied. However, 1-hour is applied during the conceptional study and initial sizing process. The wind stationary is about 10 minutes. Therefore, the mean wind speed should be properly converted for longer simulation [4].
To simulate time in transient case depends on the decay time of the motions. A full decay in all motions should be granted. For catenary mooring system minimum 600 seconds is required.
Number of seeds are depends on the concept and cite conditions. This should be high enough to give a proper characteristic response. A sensitive study is therefore is required based on the design standards stated minimum seed.
In general, the short-term wave conditions can be generated by wave spectrum for design purpose. The common wave spectrum in Norwegian continental shelf is JONSWAP for wind sea. However, in FOWT the swell can have a significant effect to the response, because of natural periods in motions. A two peaked power spectrum such as Torsethaugen which includes effect of swell recommended in an irregular sea with swell [4].

The normal sea state(NSS) in ULS design defined as a range of wave periods with associated wave heights. For a bottom fixed structure, it is possible to neglect the effect of Tp. But it is not the case in a floater which with longer natural periods. The responses might be sensitive to wave period. Therefore, in FOWT, several periods associated with maximum H_s should be considered in NSS.
For extreme sea state (ESS) or severe sea state(SSS), all points on the environmental contour should be considered. Considering only the highest H_s is not sufficient. One can consider the all wave periods combined with a higher H_s for simplifying the analysis.

The current generates current load to structure. It can introduce a significant static healing in a spar which with a long draft. The periods of vortex-induced vibration (VIV) should also be considered in structural dynamic analysis.
For the normal current model(NCM) a conservative constant current speed can be applied.
For the extreme current model(ECM) the current with 50 years return period can be sufficient. However, the response can be larger with smaller current speed because of the reduced hydrodynamic damping [3].

2.4.2 Fatigue limit state (FLS)

Unlike to the ULS, normal load-cycles have a significant contribution to the fatigue damage. Because they are more frequently happen. In principle, every load cycle which a wind turbine experienced in a lifetime can contribute to the crack grows, if they are above the fatigue limit. However, it is impossible to consider every single load case in fatigue assessment. In order to estimate the fatigue

life in a reasonable computational effort it is important to predict the load cases which is most relevant to the crack growth.
For the fatigue calculation the mean wind speed, wind directions, wind misalignment and turbulence are important parameters in wind condition. While the wave parameters such as significant wave height, peak period, wave direction and the spectral shape are important. In addition, the current parameters such as current speed, direction, and profile can also have significant effect.
The mean wind speeds to be in consideration can reduce by binning and lamping. While the sea states with a peak period closer to any of the natural periods are more relevant. The parameters are most relevant can be identified with sensitivity study or based on experience from previous projects. [6].
The most relevant DLCs for ULS:
The DLC_1.2 assumed to be the major contributor for fatigue load. Especially when the wind and wave misalignment is 90 degrees. In that case, the aerodynamics damping is zero.
The DLC_1.7 can be a case, when the current and wind directions presented opposite. Which lead to significant pitch motion. In RNA and tower design, the 10 minutes simulation with a proper number of seeds can be sufficient. While 3-hour simulation is recommended for the floater components and the mooring lines. Minimum 6 seeds are stated in the standards. However, a sensitivity study to verify the recommended minimum seeds is required [3].

Chapter 3

Theory

3.1 Extreme Value Prediction

The offshore environment contains the randomness of the nature. It exposes stochastic loads. Therefore, it is impossible to determine a load state and corresponding load effect in a future time. However, we can predict the probability of an environmental state based on historical data. Thus, the characteristic design values defined as an annual exceedance probabilities. For example, in the DNVGL-ST-0119, the USL control for design of FOWT structures defined as the 98% quantile in the distribution of the annual maximum combined load/response. [4]. It is the combined load or combined load effect that has a 50 years return period. The similar requirement also described in IEC TS 61400-3-2 [12].

To estimate a reliable characteristic design value based on limited data, we apply some statistical methods. There are several methods available for predicting characteristic loads or responses with an annual exceedance probability. Each method has its advantages over others and works well on some specific response problems.The further discussion written based on the chapter 6 and the chapter 9 of the book "Metocean Modelling And Prediction Of Extremes" [13].

In simple problems, the q-probability response directly results from the q-probability wave height, and the deterministic design wave approach works well in such problems. Stokes 5th order wave profile is the recommended deterministic wave profile that defines the wave kinematics to the actual surface [7]. We can apply this approach to the bottom fixed structures where the natural periods are much smaller.

In more complex problems where the response depends on the significant wave height, the period and the previous load history, the proper way of estimating characteristic response is to carrying a stochastic long-term analysis. A good prediction of the q-probability response should properly take the short-term variability of the response and the long-term variation in the weather condition into account. The methods are all sea state approach and random storm approach.
To extreme value prediction, it is convenient to describe long-term variation with the long-term distribution of 1-hour extremes. The time window can vary from 20 minutes to six hours. But the one hour stationery environmental state is a common practice in OWT design that specified in the design rules.

The joint probability of the environmental state including wind and waves can be written as:

$$f_{U_w,H_s,T_p}(u,h,t) = f_{U_w}(u) f_{H_s|U_w}(h|u) f_{T_p|U_w,H_s}(t|u,h) \tag{3.1}$$

Assume $x_{0.02}$ is the response that has 50 years return period. The long-term probability of exceeding this level can be written as:

$$1 - F_{X_{1h}}(x_{0.02}) = \int_h \int_t \int_u [1 - F_{X_{1h}|H_s,T_p,U_w}(x_{0.02}|h,t,u) f_{U_w,H_s,T_p}(u,h,t) dudtdh \tag{3.2}$$

$$1 - F_{X_{1h}}(x_{0.02}) = \frac{1}{N_{50,1h}} \tag{3.3}$$

Where $N_{50,1h} = 365 * 24 * 50$ is the number of 1-hour environmental states in 50 years.
Establishing the response distribution for each environmental state is an enormous challenge for a non-linear problem such as FOWT. The easiest way is running integrated time domain simulation with enough numbers of times in all the environmental states. Then, the long-term distribution of the response got as a weighted sum of the response distributions of the various environmental sates. The short-term distributions weighted based on the frequency of occurrence. Thus, the full long-term response analysis of FOWT requires a significant amount of computational time.

The most effective method that can give a reasonable estimation is the Contour Line Approach. It is a short-term approach for predicting the Long-Term response. The Figure 3.1 illustrates the environmental contour surface that has 50 years return period. In case the 1-hour extreme response distribution has a minor variation, we could neglect the short-term variation. Then the q-probability load effect can be estimated by the expected value of the maximum load effect in the environmental state whose return period is 50 years. However, the 1-hour extreme response distribution has a significant variation in most of application. Neglecting short-term variability will introduce up to 30% underestimation in a non-linear problem. We can correct it by taking a higher quantile than 50%. It is conservative to take the 90% quantile for ULS and 95% quantile for ALS in offshore structures.

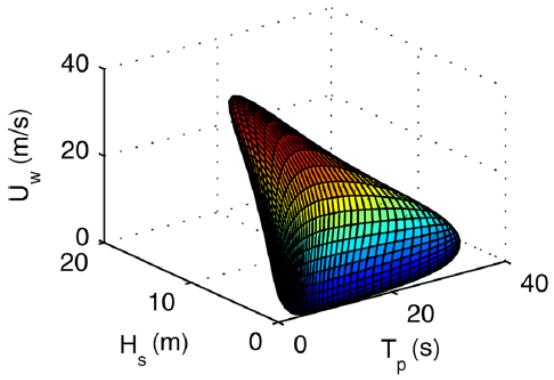

Figure 3.1: The 50-years contour surface for site 14 [10]

The Contour Line Approach with time domain simulation:

- Frist step is predicting the contour surface for the wave and wind conditions. Then we are defining the worst environmental condition on the contour surface Figure 3.1.[10]

- Second step is running (20-40) times 1-hour integrated time domain simulation to getting the maximum response in that worst environmental state. We should interpret the background environmental conditions properly in the simulation settings. The process results (20-40) maximum responses.

- Third step is to fitting the maximums to a Gumbel distribution. This will give us a maximum response distribution for that corresponding worst environmental state.

- The last step is reading the 90% quantile as a conservative prediction of the characteristic ULS load effect. 95% quantile is a good estimation for characteristic ALS load effect. To taking the short-term variation into account, we are using a higher percentile than median. One could add the short-term variation with a correction factor. The correction factor varies between 1.1-1.3.The free variable in this method is the percentile. The reliability of the result depends on an adequate correction to short-term variability.

3.2 Statistical methods

Engineers are using statistical tools to predict the extreme values. For example, to obtain the long-term environmental distributions, one is fitting the historical hind-cast data to an existing probabilistic model. In the same way, one is using the simulation extremes to get the extreme value distribution.
Selecting the right model is important. One should have an idea on why to choose that specific model. We have limited data in most practical applications. In addition, the data usually concentrated on the central part of the distribution. Several models seem to reasonable at the central part may not fit at the tail region. To have a good estimation of the extremes, fitting at the tail is crucial. Fortunately, some specific probabilistic models work well with common specific problems. For example, Gumbel distribution can model the largest out of underlying variables very well, while the Gaussian distribution suits for the mean value problem. We need a sufficient amount of sample in both cases.
Assume that Y is a variable that contains the maximum responses of the simulations; $Y_1, Y_2, ..., Y_n$. The gumbel distribution can be writen as:

$$F_Y(y) = exp\bigg(- exp\bigg(- \frac{y-\alpha}{\beta} \bigg) \bigg) \tag{3.4}$$

The fitting process is to determining the free variables in the probability models. In theory, the maximum likelihood method gives the best estimation to the distribution parameters. But it requires enormous sample size and gives inconsiderable weight on the tail part. This method is not practical for many applications. Another method of fitting is Linear Regression. It is a strait forward method that fits a strait line to the data points on the probability paper. One plots the strait line based on the square distance between points and the line itself. Thus, some people call it least square method. However, this approach gives too much weight on the data points at the low probability regions. The time-proven approach for most practical applications is the method of momentum. This method usually describes the tail part better than other two methods.
It is also important to validate how your model fitted to your data. Because we have always the probabilistic model related uncertainties and the distribution parameters related uncertainties. The goodness of the fitting influences your result. Several methods are available for this purpose. The known ones are Chi-square test and The Kolmogorov test. The probability paper can also work for the same purpose on a basic level. The advantages of this is that we will have a visual intuition about the goodness with little computational effort[13].

3.3 Gaussian surface process

The surface elevation is a stochastic process. It is only possible to measure realization of it in a certain position over a certain time period. The surface elevation process can be described as a sum of an infinite number of wave components. Assume that none of the wave component is dominating term, the surface process is a Gaussian distributed parameter according to the central limit theorem. If the underlying wave spectrum is known, one can generate surface elevation process corresponding to a specific location. The surface elevation process can be described as:

$$\xi(t) = \sum_{n=1}^{N} \xi_n sin(\omega_n t - \varphi_n) \tag{3.5}$$

In Equation (3.5), the ξ_n is amplitude and ω_n is the frequency of the n^{th} component and the φ is the random phase that varies between 0 and 2π. ξ_n can be determined with:

$$\xi_n = \sqrt{2 S_{\Xi\Xi}(\omega_n)\Delta\omega} \tag{3.6}$$

The $\Delta\omega$ is frequency resolution and equals to $\frac{2\pi}{T_s}$. T_s is simulating time.

The water particles motion under the surface are the sources of wave forces. Based on the relations between surface elevation and velocity potential, the velocity potential in deep water can be expressed as:

$$\phi(x,z,t) = \sum_{n=1}^{N} \xi_n \frac{g}{\omega_n} e^{k_n z} cos(\omega_n t - k_n x + \varphi_n) \tag{3.7}$$

The water particle velocity in x direction can be expressed as:

$$u_x(x,z,t) = \frac{\partial \phi(x,z,t)}{\partial x} = \sum_{n=1}^{N} \xi_n \omega_n e^{k_n z} sin(\omega_n t - k_n x + \varphi_n) \tag{3.8}$$

The water particle acceleration in x direction than be:

$$\dot{u}_x(x,z,t) = \frac{\partial^2 \phi(x,z,t)}{\partial x \partial t} = \sum_{n=1}^{N} \xi_n \omega_n^2 e^{k_n z} cos(\omega_n t - k_n x + \varphi_n) \tag{3.9}$$

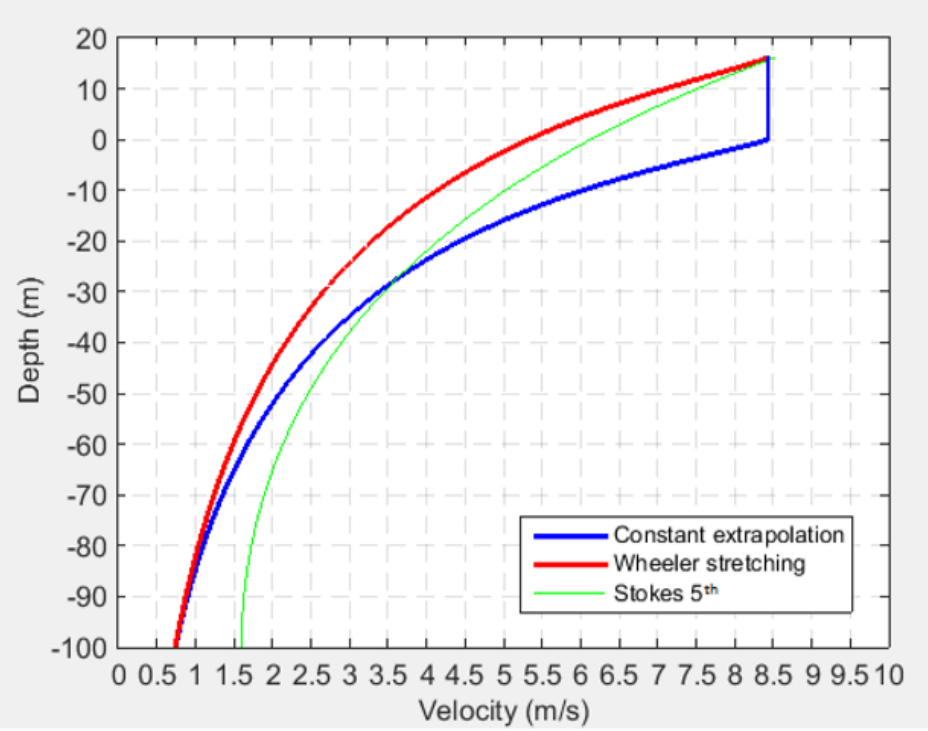

Figure 3.2: Illustration of wheeler stretching and constant extrapolation [8]

Because of the assumptions the linear wave theory valid up to mean free surface $z = 0$ and an approximation are required for positive z values. Wheeler stretching is the one that used most in practical despite of it could underestimate under the crest. The constant extrapolation is another method that used in some applications and gives too conservative result under the crest [8]. The Figure 3.2 is the illustration of the two methods.

3.4 JONSWAP wave spectrum

The commonly used standard spectrums in Norwegian continental shelf are the Pierson-Moskowitz wave spectrum for fully developed sea; the JONSWAP wave spectrum for growing wind sea; the Torsethaugen wave spectrum for combined sea. Here in this study the JONSWAP wave spectrum is used. It is a multinational measurement carried in 1968-1969 in the Southern North-Sea. As a result of this activity, the JONSWAP was founded as a standard spectrum that presents the growing

wind sea. JONSWAP spectrum:

$$S_{\Xi\Xi}(\omega) = 0.05h_s^2 t_p(1 - 0.287ln\gamma)\left(\frac{\omega}{\omega_p}\right)^{-5} exp\left[-1.25\left(\frac{\omega}{\omega_p}\right)^{-4}\right]\gamma^{exp\left[-0.5\left(\frac{\omega-\omega_p}{\sigma\omega_p}\right)^2\right]} \tag{3.10}$$

The t_p is peak period and the peak frequency is $\omega_p = \frac{2\pi}{t_p}$. The σ is 0.07 when $\omega <= \omega_p$, 0.09 when $\omega > \omega_p$. The peak factor γ can be found with:

$$\gamma = 42.2\left(\frac{2\pi h_s}{g t_p^2}\right)^{\frac{6}{7}} \tag{3.11}$$

3.5 Morrison's equation

The Morrison's equation is a well known and time proved equation in the marine engineering field. It gives reasonably good prediction to the wave loads on a submerged cylinder structure in small diameter. The cylinder diameter should be 5 times smaller than the wavelength. Morison equation applies for monopile, jacket, jack-up, spar and some semi-submerged wind turbine support structures [8].
The load on a unit section with Morrison equation:

$$f(z,t) = f_m(z,t) + f_d(z,t) = \frac{1}{4}\rho C_m \pi D^2 \dot{u}(z,t) + \frac{1}{2}\rho C_d D u(z,t)|u(z,t)| \tag{3.12}$$

Integrating the Equation (3.12) over the submerged part to get the time varying wave loads on the structure:

$$F(t) = \int_{-d}^{\xi(t)} \frac{1}{4}\rho C_m \pi D^2 \dot{u}(z,t)dz + \int_{-d}^{\xi(t)} \frac{1}{2}\rho C_d D u(z,t)|u(z,t)|dz \tag{3.13}$$

The Morrison equation is the sum of the drag term and the mass term. The drag term is proportional to the square of the water particle velocity and has the drag coefficient C_d. The water particle acceleration proportional inertia term has a corresponding inertia coefficient C_m. The C_d and C_m are depends on Reynolds number and Keulegan-Carpenter number [8].

Chapter 4

The numerical model

4.1 RNA

Parameter	Values
Rated power	10MW
Rotor orientation and configuration	Upwind, three blades
Rotor, hub diameter	178.3 m, 5.6m
Hub height	119.0m
Cut-in, rated, cut-out wind speed	4.0 m/s, 11.4 m/s, 25.0 m/s
Cut-in, rated rotor speed	6.0 rpm, 9.6 rpm
Overhang, shaft tilt, pre-cone	7.1 m, 5.0 grader, -2.5 grader
Rotor, nacelle, tower mass	230.7 t, 446.0 t, 628.4 t

Table 4.1: DTU 10MW reference wind turbine [9]

4.2 Spar

Parameters	Spar 1
Draft (m)	120.0
Elevation to tower base above SWL (m)	10.0
Depth to top of taper below SWL (m)	4.0
Depth to bottom of taper below SWL (m)	12.0
Diameter above taper (m)	8.3
Diameter below taper (m)	12.0
Mass including ballast (kg)	1.18E+7
Displacement (m3)	1.31E+4
Moment of inertia about CoG (kgm2)	6.53E+9
Vertical CoG below SWL (m)	94.7
Vertical CoB below SWL (m)	62.0

Table 4.2: Properties of the model [9]

4.3 Mooring lines

The model has 3 catenary lines. For convenience in modeling in SIMA, the mooring lines modeled with constant properties up to the fairleads. The yaw stiffness applied as a spring [9]. The specific details given in the Table 4.3.

Radius to anchors	855.2[m]
Unstretched mooring line length	902.2[m]
Equivalent mooring line mass dencity	155.4[kg/m]
Equivalent mooring line axial stiffeness	$3.84 \times 10^8[MN]$
Fairlead depth below surface	77.2[m]
Yaw spring stiffeness	$1.48 \times 10^8[Nm/rad]$

Table 4.3: Specifics of the mooring system [9]

4.4 The numerical model in SIMA

The numerical model used in the current study is provided by Erin E. Bachynski in the model subject Integrated Dynamic Analysis of Wind Turbines. It is a model for running a coupled nonlinear aero-hydro-servo-elastic analysis in SIMA. SIMA is a coupled nonlinear time domain simulation program developed by SINTEF Ocean. It couples two codes Riflex and Simo [9].Specific details for the modeling given in the Table 4.4

Parts	Modeled element	Commend
Spar buoy	six-dof 3D	Wave forces: Potential flow theory; Viscouse forces: drag term in Morison's equation;
The mooring lines	two-dof bar	Morison's equation;
Tower	six-dof beam	Drag forces;C_d=0.7;
Blades	six-dof beam	Aerodynamic loads: BEM with corrections*
The controller	JAVA code	PI controller**

**Glauert correction,Prandtl hub, tip loss factors, dynamic stall, dynamic wake, skewed inflow, tower shadow effect;*
***Modifying the proportional and intergral grains above the rated speed to avoid pitch motion instability*

Table 4.4: How the model modeled [9]

4.5 Cite Conditions

The characteristic response for ULS design estimated as the expected value of the maximum response in worth environmental state which has a 50 years return period [4]. The wind and wave assumed to be stationary in one hour in fixed structures [5]. This assumption applied in floating wind turbine in initial sizing and conceptional design process. [3]

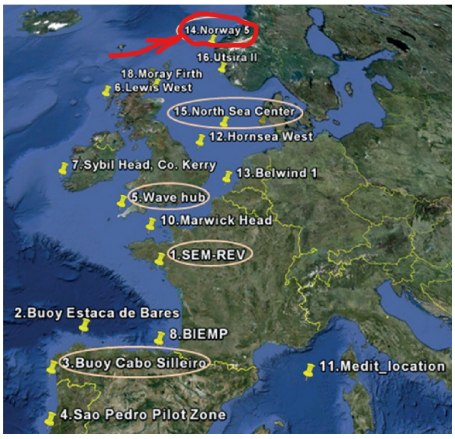

Figure 4.1: 18 European offshore sites on the map [10]

The environmental contour surface are extrapolated from long-term joint distribution of the wind and wave. In principle we should consider all the points on the environmental contour[6]. However, in current study the major interest is in finding a short-simulation approach to save computational effort. Therefore, the environmental state with maximum H_s on the contour surface are chosen to carry further study. The site selected based on the properties of the model. The locations of the sites are presented in Figure 4.1. The red circle is the selected site for simulation in this project.The parameters of the environmental state are presented in table Table 4.5.
The Norway 5 from the list was selected because the 202m water depth is sufficient for a spar that has a 120 meter draft. Further, the average wind power density in Norway 5 is high, and have potential for further wind turbine projects [10].

Parameters	Values
$H_{s_{50}}$	15.6[m]
$T_{p_{50}}$	14.5[s]
$U_{w_{50}}$	31.2[m/s]

Table 4.5: Environmental condition on the 50-year contour surface conditioned with maximum Hs [10]

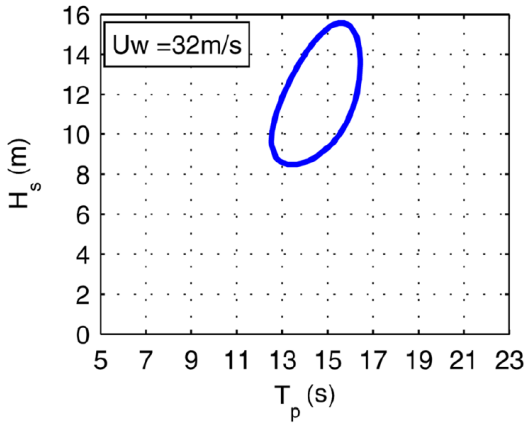

Figure 4.2: The 50 years contour for $U_w = 32m/s$ [10]

The parameters are estimated by analyzing the 10 years of numerical hind-cast data. The data were provided by National Kapodistrian University of Athens(NKUA). The data fitted in to two-parameter Weibull distribution and the hybrid Lonowe model for extrapolating the 50-years environmental contour. The 50 years contour for $U_w = 32m/s$ given as illustration Figure 4.2.
The U_w is the wind velocity at 10m over mean water surface level and should be converted to wind speed at hub height [10].

$$U_{hub_{50}} = U_{w_{50}} \left(\frac{z}{10} \right)^{0.1} \tag{4.1}$$

Chapter 5

Phase I

5.1 Method

Ultimate load analysis requires a minimum 5 hours simulation [6]. This is a time-consuming process. The stochastic wave can be generated in a scant time. However, solving the dynamic equation in time domain step after step is time consuming. Thus, there is a need for simpler simulation method. If the wave is dominant, a few short simulations at maximum wave maximums may give sufficient result. This method probably can reduce simulation time in some DLCs without losing the reliability of the result.

The purpose in this phase is to create the maximum response distribution of 1-hour simulation as a reference; further, investigating where the maximum responses are happening.If the wave is the primary contributor as assumed, the peak points of the surface elevation expected to be the relevant points. We focused on the extreme response at tower base in this study. Because of the alignment in wave and wind directions, the fore-aft moment FA_moment at tower base is expected to be the dominant ULS response.

Design Situation	Parked
Wind condition	EWM (Extreme Wind speed Model)
Wave	ESS (Extreme Sea State), $H_s = H_{s,50}$
Functionality	misalignment
Sea current	ECM (Extreme Current Model), $U = U_{50}$
Water level	EWLR (Extreme Water Level Range)
Type of analysis	Ultimate Strength
Partial safety factor	Normal
Other conditions	Yaw misalignment of ± 8
	Possible yaw slippage

Table 5.1: DLC_6.1 [6]

The DLC 6.1 from the DLC table in DNVGL-ST-0437 implemented with some adaptations (ref: DNVGL). Such as the effects of the turbulence, misalignment and the current are neglected. Further, 100 times one hour simulation carried in SIMA to have a proper distribution of the maximum response of 1-hour simulation. The Table 5.1 and Table 5.2 specified the DLC 6.1 and the simulation setup for current investigation.

The wave peaks can be described by wave height or crest height. Which of them is most relevant to maximum responses? That should be answered before proceeding. Therefore, the probability of the maximum FA follows the maximum peaks in each wave parameters are calculated. Because of the delay is unknown in this stage, the calculation carried at varied time points after the maximum peak. In order to understand the behaviors and relations of the responses, the same study is con-

Simulation parameters	Simulation length	4000s
	The pre-simulation time	400s
	Simulation time step	0.005s
	Response time step	0.1s
Wave condition	Jonswap_3 parameter	$H_s = 15.6$
		$T_p = 14.5$
		$\gamma = 3.099$
Wave kinematics	Kinematics at static positions.	
	Constant stretching	
Turbine condition	Parked*	
	Blades feathered	
Wind conditions	Stationary uniform	V=40m/s**

Table 5.2: Simulation setup in SIMA

** The parked condition in SIMA achieved with following steps:*

- *Creating master slave condition between supernodes towerup and sh-sn1; stopping the spinning of the rotor.*
- *Blades feathered by changing the twist angle; adding -90 degree to each blade section.*
- *Editing the controller; set the minimum pitch angle=0 and maximum pitch angle = 0.1 (a tiny number close to zero).*
- *The BEM method is not suitable for parked condition; Turn off induction calculation.*

*** The wind speed at hub height.*

ducted to other responses as well.

The crest and trough determined by dat2tc function from Wafo toolbox (ref: wafo). Then, the maximum wave height is defined with zero up-crossing rules. The index for maximum wave height is the index for the corresponding crest.

To investigate the connection between the wave and the maximum FA, the statistics of the corresponding H are of interest.

To suggest the potential possible simplified approaches, we compared the cumulative probability distributions of the maximum FA and the responses of the maximum waves. It is not practical to include higher order maximums, thus we take only the first and second maximum waves into account. The response of the maximum wave height studied as an ultimate approach. It is a simple solution. The greater response of the first and the second highest wave considered as an alternative approach. This approach requires twice more simulation time, but we expect it to be more precise. The purpose of the ultimate load analysis is a reasonable estimation to the characteristic response. To characteristic value estimation, the standard suggests using the expected value of the maximum response distribution in the worst environmental state. Thus, the maximum response distribution of 1-hour simulation compared with the two distributions of the maximum wave height responses.

The simulation results are a realization of the stochastic response. The sample size is small. Therefore, the sample distribution cannot describe the response process well. Thus, we fitted the 100 simulation results into the Gumble distribution. Both the linear regression and the method of momentum used to determine Gumbel parameters [13]. Besides that, we carried the Gumbel analysis on 30 random simulations to check the possibility for smaller sample size.

5.2 Result

The Figure 5.1 shows the cumulative probability of the occurrence of maximum response. In plot (a) the occurrence probability calculated in each second after wave maximums. The zero in X-axis refers to the time point that the maximum wave heights/crest heights show up. Almost 50% maximum FA-moment occurred in five seconds after the wave heights, while 40% maximum FA-moment related to the maximum crest heights. The plot (b) presents the cumulative occurrence probability of the maximum FA-moment at the varied order of the maximums. The 1^{st} order refers to the maximum wave; the 2^{nd} order refers the second maximum wave and so on. The study carried up to the 5^{th} order wave maximum. The 95% maximum FA-moments occurred at the top five wave height, while it is 75% in case at crest height. Based on the study, the maximum FA-moment seems more probably happens at maximum wave height than crest height; the response delay is about 2-4 seconds.

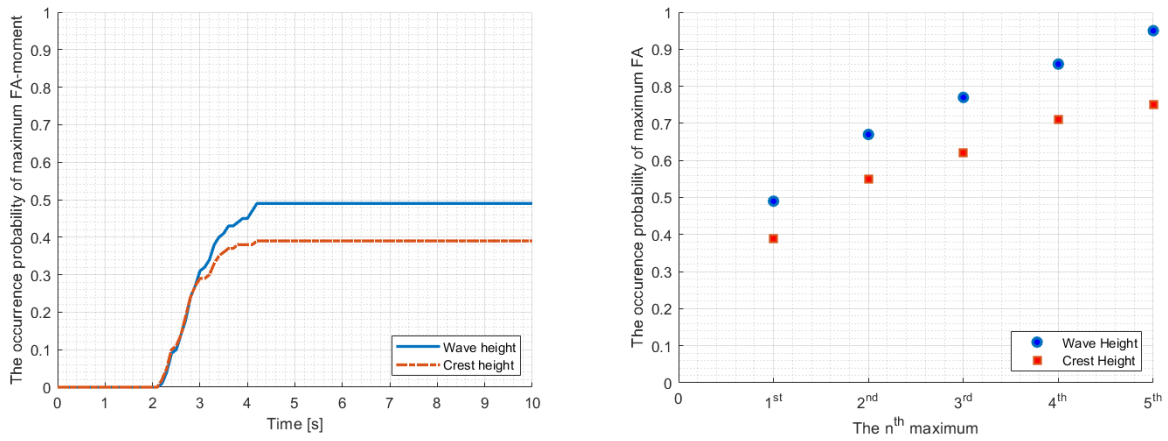

(a) In time (b) The order of maximum wave height

Figure 5.1: The cumulative probability of occurence - maximum FA-moment

In plot (a) the time starts where the wave height/crest height occurred. Nearly 50% maximum FA-moment is occurred in five seconds after the maximum wave height. The 95% maximums of FA-moment occurred in six seconds after the top five wave heights, while it is 75% if we use the crest height. Based on the 100 simulations, the maximum FA-moment seems more related to wave height than crest height.

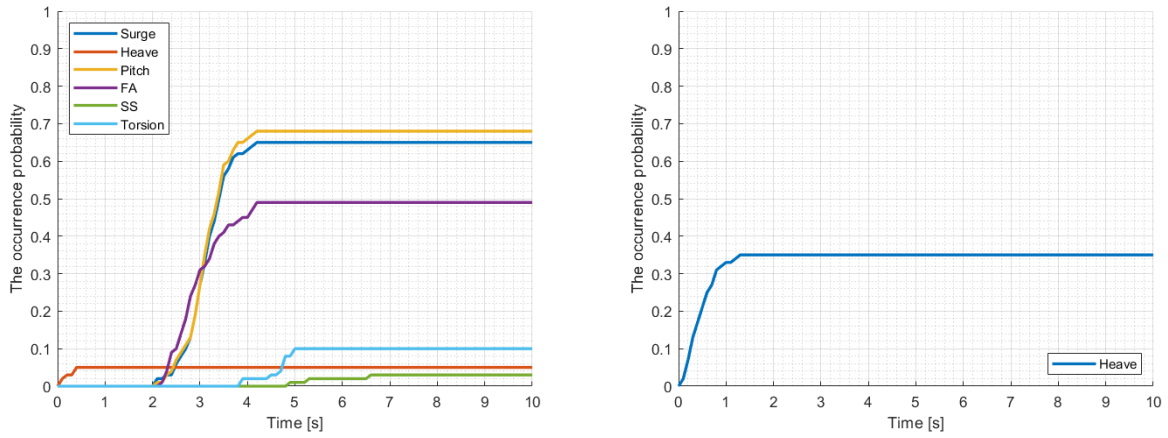

(a) (b)

Figure 5.2: The cumulative probability of occurence in time

65% maximum surge and 68% maximum pitch has happened in five seconds after the maximum wave height. Further, 5% maximum heave motion occurs in one second after the maximum wave height, while a majority (35%) occurs one to two seconds before. The maximums of other motions seems not really depends on the wave condition.

The Figure 5.2 illustrates the cumulative probability of occurrence of some other motions and

responses at tower base. The zero point on the X-axis refers to the occurring time of maximum wave height. Over 65% maximum surge and pitch motions occurred in five seconds after the maximum wave height, but the maximum SS-moment and torsion seems not relevant to wave heights. 35% maximum heave motions occurred one to two seconds before the maximum wave height.

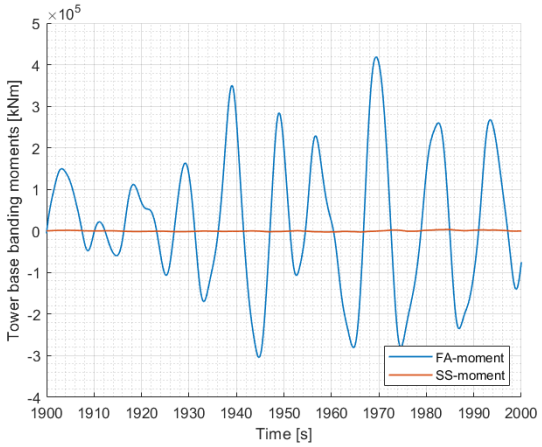

(a) Comparing the tower base banding moments

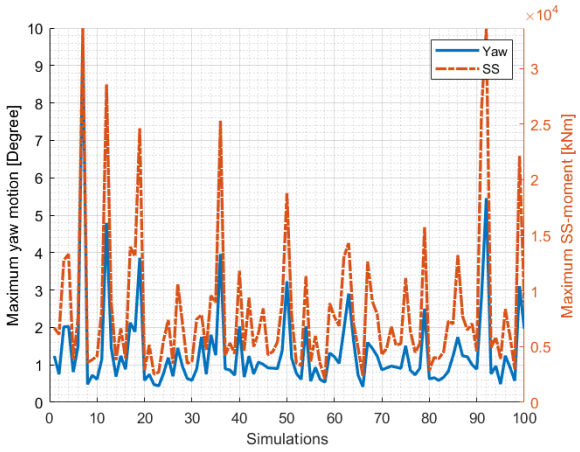

(b) The relation between maximum yaw and maximum SS-moment

Figure 5.3

The plot (a) is an interval on the response time series in simulation 81. The peak in the figure is the response of the maximum wave height and equals to 4.1885×10^5. *Further, the maximum SS-moment in the same simulation is* 4.0292×10^3 *and over 100 times smaller than the peak FA-moment. Thu, the FA moment is the dominant tower base banding moment. The plot (b) is illustrating the relation between the SS-moment and yaw motion. Larger yaw motions corrosponds to larger SS-moments.*

The plot (a) in the Figure 5.3 comparing the time series of FA-moment and SS-moment at tower base. The series results from simulation 81. The peak FA-moment is the response of maximum wave height and equal to 4.1885×10^5; it is 100 times larger than maximum SS moment in the time series. The maximum torsion moment in the same simulation is 573[kNm]. To sum up, the FA-moment is the dominant response at tower base.
The plot (b) in the Figure 5.3 illustrating the relation between global yaw motion and the SS-moment. The simulations with larger maximum yaw motion results a larger maximum SS-moment. This shows the nonlinear relations between yaw and internal moments. At the same time, it shows the variation of SS-moment and yaw; the 100 maximum yaw varies from 0.4 degree up to 10 degree; the 100 maximum SS-moment varies from 2.1×10^3 to 3.4^4. Further, the mean maximum yaw is a 1.36 degree, while the mean SS-moment is 8.2×10^3. Only three simulations results a maximum yaw larger than four degrees.In the 21 cases, the SS-moment is over 10^4 which corresponds to approximately 2% of the maximum FA-moment. The largest maximum SS-moment corrosponding to approximately 7% of the maximum FA-moment. We used 400 seconds of initialization time in 1-hour simulations, and the transient responses may be the reason for the special cases. The yaw motion and SS-moment expected to take longer for equilibrium in dynamic calculation. We will discuss more about that in the second phase.

The Figure 5.4 illustrating the nonlinear relation between global motions and windspeed. The plots show a part of the time series in pitch/yaw motions and Y/Z-components of the wind speed at hub height. The time series are results of simulation 81. The input wind in the simulation is uniform wind, which refers to a constant wind speed. However, the X-component of the wind speed at hub height has oscillation. The oscillation is resulted by the yaw and pitch motions. They change the relative direction of the wind speed to rotor plane; generate Y-component and Z-component of the wind speed. The Y-component of the wind speed is the major contributor of the SS-moment at the tower base.

The Figure 5.5 shows the distribution of the maximum FA-moment respect to the corresponding or-

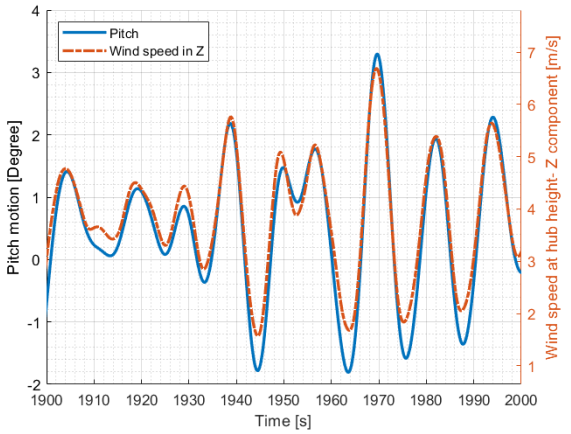

(a)

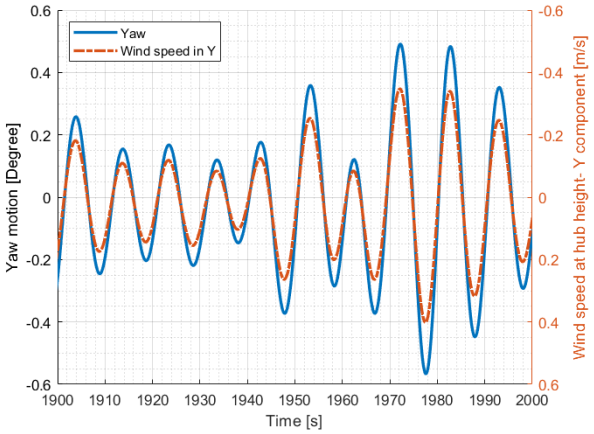

(b)

Figure 5.4: The relations between the pitch/yaw motion and the wind speed at hub height in Z/Y-direction

The yaw motion creates Y-component of the wind speed; The pitch motion creates Z-component of the wind speed. This creates a variation in the X-component of the wind speed, despite the source wind is uniform/constant wind. The Y-component of the wind speed is the source of SS-moment. Because the yaw motion is slight in our problem, the resulted SS-moment is negligible.

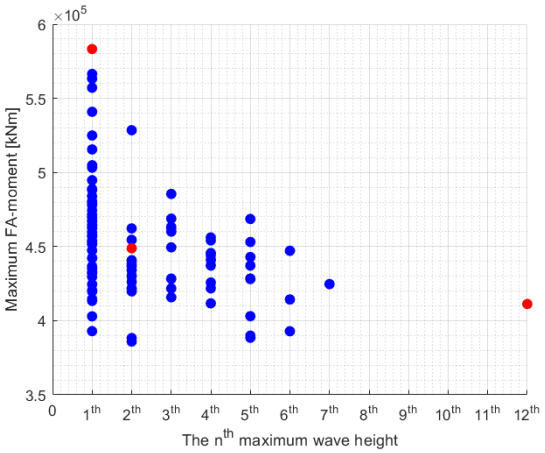

(a) The maximum FA-moments

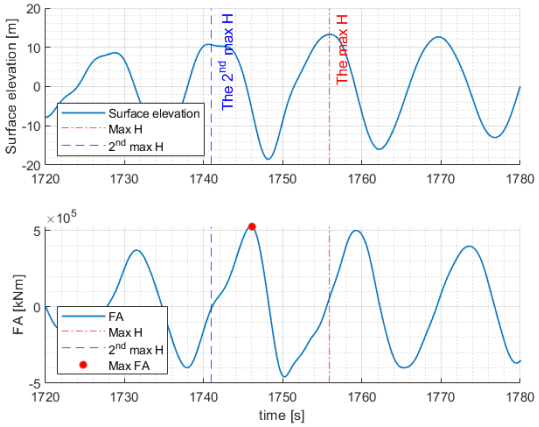

(b) Diving to the time series of the special case: simulation 32

Figure 5.5: The distribution of the maximum FA-moment respect to the corrosponding order of wave height

The maximum FA-moments larger than $4.8548 \times 10^5[kNm]$ *occurs in six seconds after the maximum wave height except from the simulation 32. In simulation 32, the first and the second maximum wave heights are one after another. The three red points refer to the three simulations that worked with in the transient time analysis.*

der of wave height. The maximum FA-moments larger than $4.8548 \times 10^5[kNm]$ occurs at maximum wave height. The simulation 32 is one exception where the maximum and second maximum wave heights happened close to each other. The respective time series of simulation 32 is given in plot (b). 99 maximum FA-moments related to the top seven wave heights while one exception relates to 12^{th} order maximum wave height. The three red marked simulations are chosen to work with in transient time study.

The blue curve in Figure 5.6 shows the distribution of maximum FA-moments in 100 1-hour simulations. It is the reference distribution which refers to the short-term extreme response distribution in the worst environmental state that has a 50 years return period.The standards recommended using the expected value of this distribution as characteristic design value. The red curve is the

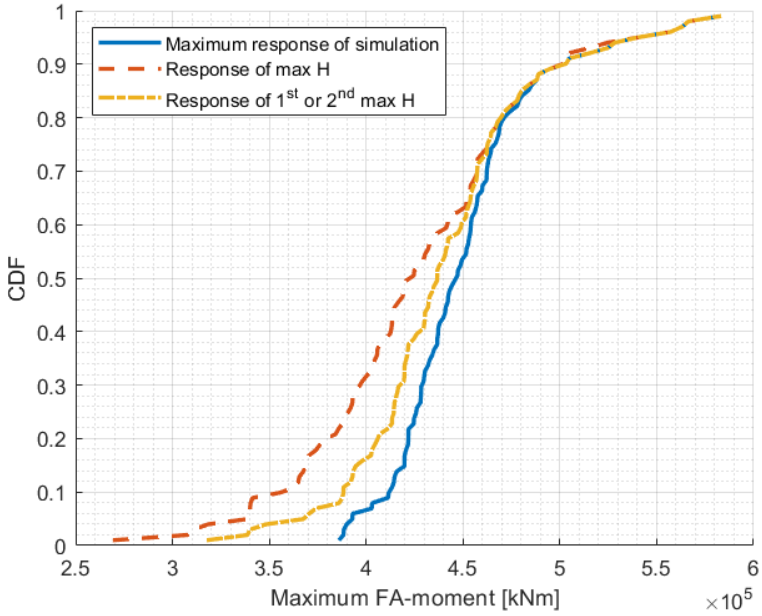

Figure 5.6: Comparing the maximum response distribution with the response of maximum waves heights

The maximum response refers to the maximum FA-moments from 1-hour simulations. The response of max H refers to the maximum FA-moment of the six seconds interval after the maximum wave height. Correspondingly, the response of $1^{st}/2^{nd}$ max H is the maximum FA-moment of the two six seconds intervals after the first and second maximum wave height. The top parts of the distributions are converging to each other.

distribution of the maximum wave height response. It refers to the maximum FA-moments in the six seconds interval after maximum wave height. The yellow curve, on the other hand, is the response distribution of $1^{st}/2^{nd}$ maximum wave height. It refers to the maximum FA-moments in the two six seconds interval follows by the first and second maximum wave height. Over the 65% quantile of the distributions has tiny differences while the variations are large at the smaller maximums. The 50% quantile The distributions have differences of approximately 6% and 2% compare to the reference.

The Figure 5.7 shows the goodness of the fitting to Gumbel model. The three distributions are fitted to Gumbel model. The model parameters are estimated by both the least square method and the method of moments. On the probability papers, the samples are not shaped a perfect strait line. It means the fitting would introduce some uncertainties. However, in the sample distributions the fitted models describes the sample distribution well and should work for our purpose in this study. In the end, the method of moments is chosen for further work.

The three Gumbel models fitted with the method of moments compared in the Figure 5.8. The black curve is the fitted maximum response distribution of 1-hour simulations witch is the reference. The blue curve is the fitted distribution of the response of maximum wave height; the 50%-quantile is 6% smaller than reference. The red curve is the fitted distribution of the response of $1^{st}/2^{nd}$ maximum wave height; the 50%-quantile is 3% smaller than reference. The fitted distributions with smaller sample size presents some tiny changes, but should still work for the purpose. A closer comparicing coming in the with specific numbers.

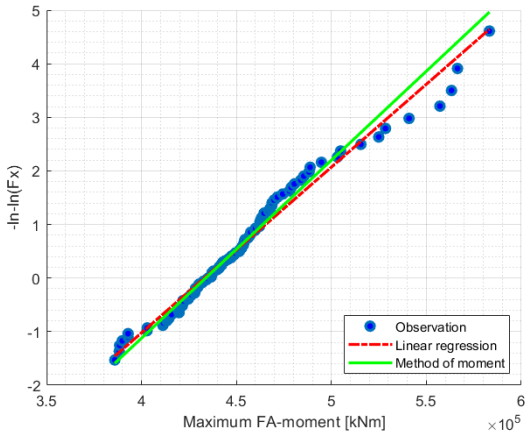

(a) The maximum FA-moment

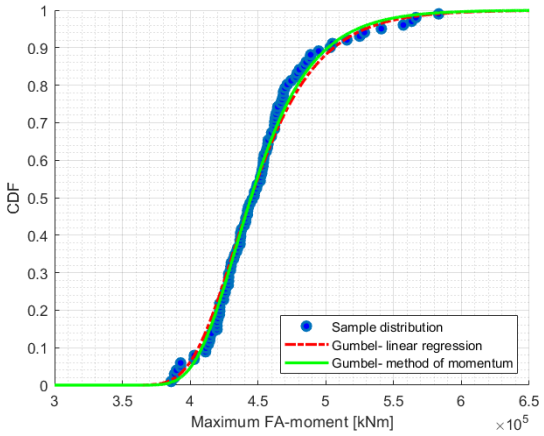

(b) The maximum FA-moment

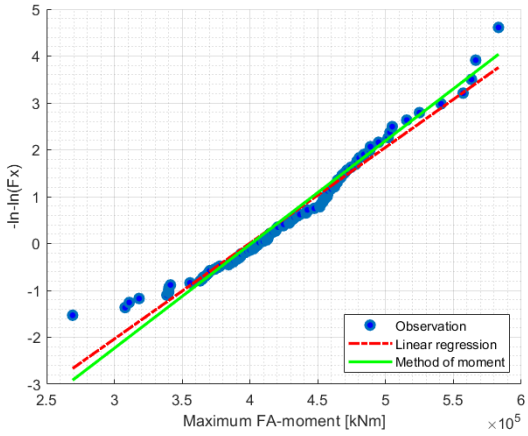

(c) The response of H_{max}

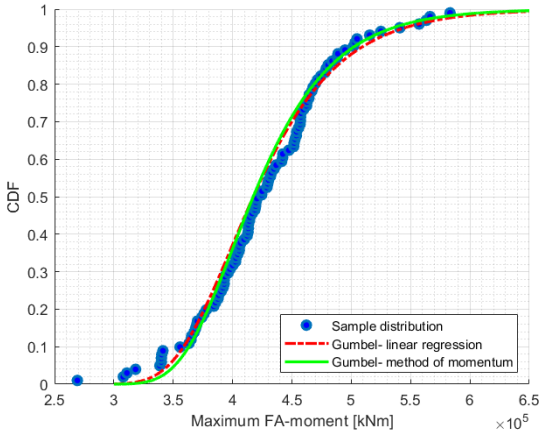

(d) The response of H_{max}

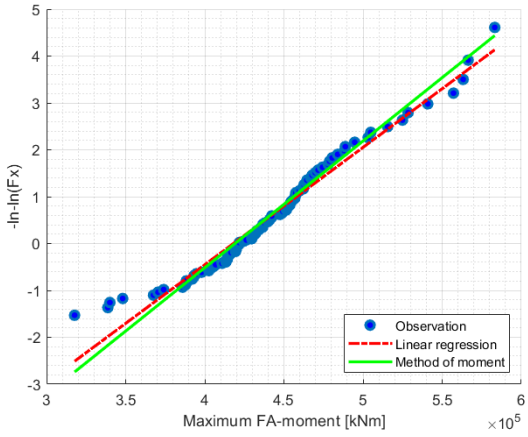

(e) The response of $1^{st}/2^{nd}$ H_{max}

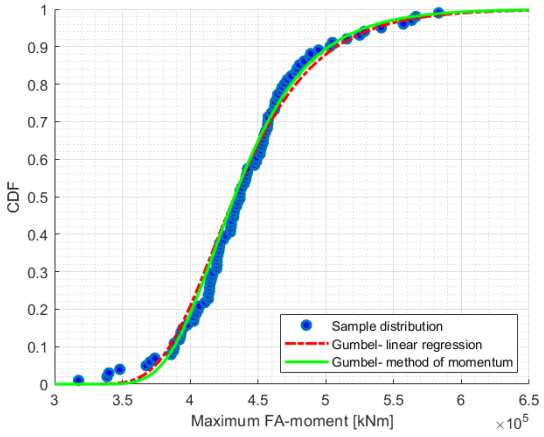

(f) The response of $1^{st}/2^{nd}$ H_{max}

Figure 5.7: Test the goodness of the Gumbel model on probability paper;Fitting to the sample distribution

The samples are not a perfect strait line on the Gumbel probability paper. Thus, it is expected to have some fitting related uncertainty. However, the model fits well to the sample distribution and works for our purpose in this study.We are interested in the expected value of the distribution.

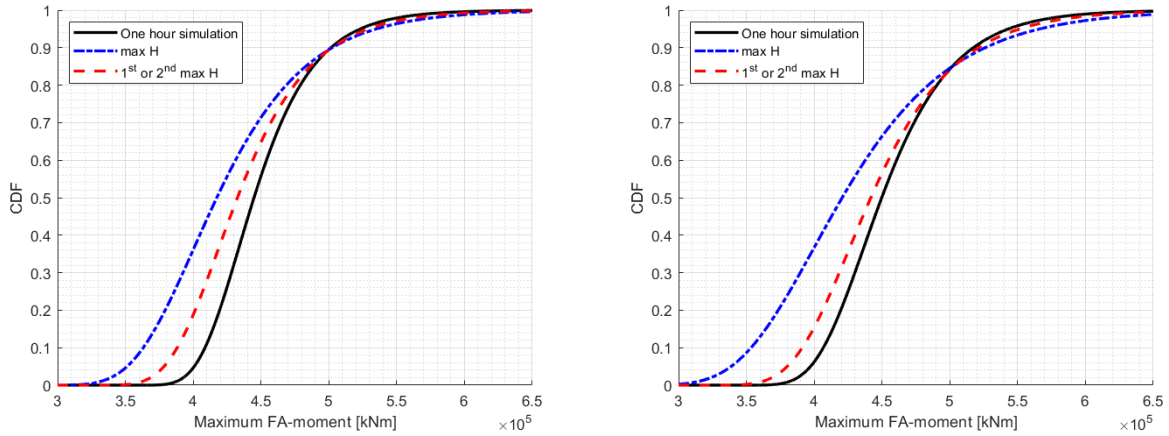

(a) With 100 simulations

(b) With random 30 simulations

Figure 5.8: Comparing the three Gumbel models

To estimate the model parameters, we used the method of moments. This method compromises the weight on the tail data and usually describes the tail better than other methods. In the 50% quantile, the response of the maximum wave height is 6% less than the maximum FA-moment. Including the response of 2^{nd} maximum wave height, the difference is about 3%.

	FA_{max}[kNm]	$FA_{H_{max}}$[kNm]	$FA_{1^{st}/2^{nd}H_{max}}$[kNm]	Difference
Sample distribution	445618	420511	436608	5.6% - 2.0%
Gumbel distribution	444800	417400	432600	6.2% - 2.7%
Expected value	451170	426910	440410	5.4% - 2.4%

Table 5.3: Comparing the 50%-quantile of the three distributions

FA_{max} = the maximum FA-moment of 1-hour simulations; it is the reference.
$FA_{H_{max}}$ = the response of maximum wave height; maximum FA-moments in a six-seconds interval at the maximum wave height.
$FA_{1^{st}/2^{nd}H_{max}}$ = the response of $1^{st}/2^{nd}$ maximum wave height; the maximum FA-moments in two six-seconds interval at the first and second maximum wave heights.

5.3 summary

The maximum FA-moment seems more related to wave height than crest height Figure 5.1. The 95% maximum FA-moment is the response of top five wave heights, while 75% maximum FA-moment is the response of top five crest heights.

The delay presented in the motions and responses in the model is about 2-5 seconds. In 99 simulations the delay in FA-moment presented in five seconds. In one exceptional case, the delay slightly larger than five seconds, and the six-seconds interval is, therefore, applied throughout the study. Pitch and surge motion in the model are more related to the maximum wave height. The yaw motion, torsion and SS-moments seems not the direct result of the extreme wave loads. They seem more related to the coupled motion Figure 5.2.

The global Yaw motion results Y-component of the windspeed at hub height. Therefore, the SS-moment at tower base larger in floaters than bottom fixed structures. However, the yaw motion is slight in our case and SS-moment can be neglected in ULS check at the tower base Figure 5.3. The presented torsion moment in the model is small.

The maximum of maximum FA-moments occurs in six seconds interval at the maximum wave height. One exception is the simulation 32 witch maximum wave height appeared 15 seconds after the second maximum wave height. The largest response in this simulation occurred in between maximum and second maximum wave height. The investigation shows that the most critical responses are related to maximum wave height.

The response distributions compared in Figure 5.6. The distributions converge above the 50% quantile and the difference become tiny above 65% quantile. The fitted Gumbel distributions crossing in approximately 80-90% quantile Figure 5.8b.

Chapter 6

Phase II

6.1 Method

The second phase is investigating the minimum reasonable time for initialization. It is the transient period; the time used for the transient effects to disappear in the dynamic calculation. It depends on the applied software codes and the controller algorithm. The transient period is longer for floating structures than fixed ones, because of the stronger nonlinearity and coupling effect in the response. Therefore, the Spar structures expected to need longer simulation to get the correct response. The recommended transient period for floaters is minimum 600 seconds [5]. However, it can be shorter in our case where the blade pitch angel set to be zero in advance. We do not want to simulate longer than it is necessary. Thus, it is important to determine a minimum pre-simulation time that can produce the response with an acceptable accuracy.

Seed	200	193	181
H_{max} shows up at [s]	2074.4	2965.9	1966.9
$FA_{H_{max}}$ shows up at [s]	2077.1	2970.2	1969.4
Starting time* [s]	1874.4 - 1074.4	2765.9 - 1965.9	1766.9 - 966.9
Simulation length** [s]	206 - 1006	206 - 1006	206 - 1006

Table 6.1: The transient time analysis

H_{max} = maximum wave height.
$FA_{H_{max}}$ = response of maximum wave height; the maximum FA-moment in the sex-seconds interval starts from the index of maximum wave height.
** the aim is to simulate the six-seconds interval that starts from the index of maximum wave height.*
*** the simulation length = the six-seconds interval starts from the index of maximum wave height + initialization period which varies from 200 to1000 seconds.*

In order to identify the reasonable initialization period, nine varied simulation-length are tested with three seeds. The seeds are 200, 193, 181 and they marked with red in **??**.They are chosen based on the corresponded maximum FA-moments. The first seed is responsible for the largest FA-moment of all 100 simulations. The second seed produced a maximum response that related to the 12th maximum wave height. With the last seed, the maximum FA-moment is the response of second maximum wave height. The nine simulation-length are 206s, 306s, 406s, 506s, 606s, 706s, 806s, 906s and 1006s. The simulations are started X00 seconds before the maximum wave height and carried for X06 seconds. Actually, the results in last 6 seconds is in prime interest, because the response of the maximum wave height expected to happen in this 6 seconds Figure 5.1. The result with short simulations compared with the reference. The reference is the corresponding maximum wave height response in the 1-hour simulation.

The SIMA settings are kept as in Phase-I except from the simulation length and the starting time.The surface elevation time series are generated for a full 1-hour simulation, while the dynamic calculation started at that specified starting time in each simulation. Total 27 simulations are

carried.
The new parameters listed in Table 6.1:
The short simulations are unrequired to produce exactly the same result. In principle, if the short simulation carried long enough, the FA-moments in the six-seconds interval are equal; the difference become zero. However, in the early phase of the design process, we are expecting to estimate a reasonable characteristic load effect. 1% to 2% difference can be accepted for an increase in the simulation speed. It is a slight error compared to the other uncertainties that affects the estimations.

The result of the study presented in a plot. The varied simulation length listed in the X-axis, and the difference in the Y-axis. The difference presented in a percent value that calculated with Equation (6.1).

$$d = \frac{FA_{H_{max},406s} - FA_{H_{max},1h}}{FA_{H_{max},1h}} * 100\% \tag{6.1}$$

Where: d = difference in percent.
$FA_{H_{max},406s}$ = the response of the maximum wave height with 406s simulation where 400 seconds is pre-simulation time.
$FA_{H_{max},1h}$ = the response of maximum wave height in 1-hour simulation; the reference.

In order to investigate the transient behavior in other responses, the response time series are studied. The simulation time series with seed-200 is chosen to work with. The short simulation is carried in the six seconds time interval plus pre-simulation time. The simulated part of the surface elevation is the corresponding interval of the 1-hour surface realization. Therefore, the surface elevations used in short simulations should be matched exactly with the reference surface elevation. It shows whether the timing of the study is correct. An illustration of the FA-moment time series also in intererst, for visualising the initialization period. Further, the pitch and yaw motions are studied; it is interesting to investigate how long the pre-simulation time should be in those motions.
To validating the result, the reasonable initialization time based on the three seeds tested on all the 100 seeds. The results are compared with the reference. The reference here is the response of maximum wave height in 1-hour simulation. The results of the short simulation is the maximum FA-moment in the simulated six-seconds interval. Actually, the process is an expansion of the three seeds to 100 seeds, but with specific simulation length. The results visually presented in plots with actual values and the differences in percent. This comparing give us a general idea about how large uncertainties expected to have with that specific pre-simulation time.
Further, the distributions of the 100 short-simulation results compared with the reference distributions which is full 1-hour simulation results. Specifically, the result distribution of the short-simulation at wave height compared with the response distribution of maximum wave height; the result distribution of the short-simulation at1st/2nd maximum wave height compared with the response of 1st/2nd maximum wave height. Finally, the distributions fitted to Gumbel distribution for smoothing.

6.2 Result

The [first plot] illustrates how long time it needs for an initialization for dynamic calculation. The X-axis is the nine simulation lengths while Y-axis is the difference between short simulation result and reference. The short simulations aim to simulate the six-seconds time interval starts from the index of maximum wave height in 4000-seconds surface elevation time series. Each seed used in nine short simulations which has 200-1000 seconds of pre-simulation time. Further, the maximum FA-moment in the six seconds interval counted as the result of the short simulation.
The reference, on the other hand, is the maximum FA-moment in the same six seconds interval in a full 1-hour simulation; the response of maximum wave height in a 1-hour simulation. Each seed has a reference.
For example, the reference value for the seed 200 is 5.8321×10^5 and occurs at 2077.1[s]. Further, it is the response of the maximum wave height that occurred at 2074.4[s] in full 1-hour simulation. There is a 2.7 second delay. In the 4000 seconds timeline, the 406 seconds simulation is started at

Seed	200	193	181
$FA_{max,1h}$ [kNm]	5.8321×10^5	4.1126×10^5	4.4884×10^5
H_{max} [m]	30.4	25.9	24.4
H_{max} shows up at [s]	2074.4	2965.9	1966.9
$FA_{H_{max}}$ [kNm]	5.8321×10^5	4.0253×10^5	4.1885×10^5
$FA_{H_{max}}$ shows up at [s]	2077.1	2970.2	1969.4
$FA_{H_{max},406s}$ [kNm]	5.8546×10^5	3.2245×10^5	4.1572×10^5
The difference* [%]	0.39	0.88	-0.39

Table 6.2: The transient time analysis

$FA_{max,1h}$ = the maximum FA-moment of 1-hour simulation.
H_{max} = maximum wave height.
$FA_{H_{max}}$ = the response of maximum wave height; the maximum FA-moment in the six-seconds interval at maximum wave height. $FA_{H_{max},406s}$ = the result of 406-seconds simulation; the maximum FA-moment in the six-seconds interval at maximum wave height with 400 seconds initialization time.

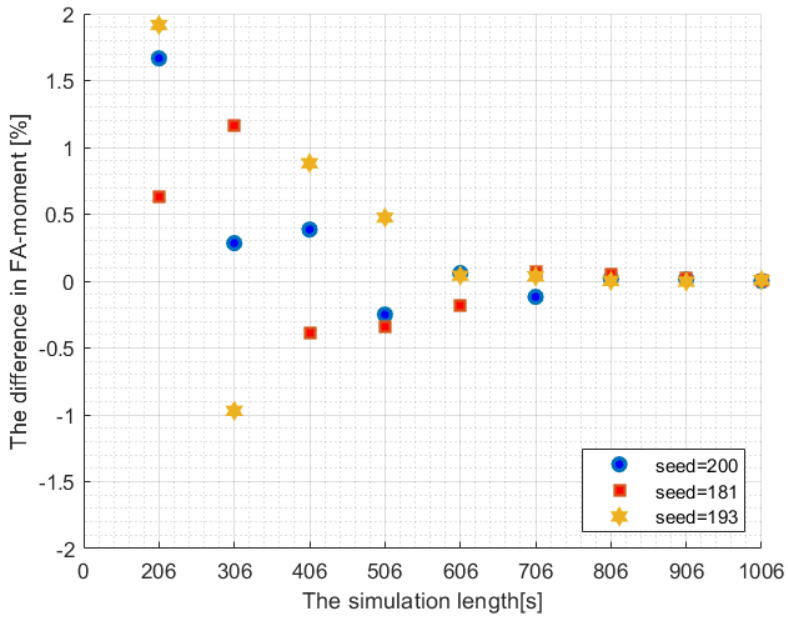

Figure 6.1: The transient time analysis

The X-axis is the nine simulation lengths while Y-axis is the difference between short simulation result and reference.
The short simulations aim to simulate the six-seconds time interval starts from the index of maximum wave height in 4000-seconds surface elevation time series. Each seed used in nine short simulations which 200-1000 seconds pre-simulation time.
The reference is the maximum FA-moment in the same six seconds interval in a full 1-hour simulation. Each seed has a reference.
The 406 seconds simulation produced a reasonable result with less than 1% difference in all three cases; the 606 seconds simulation produce a better result at the price of 30% more computational afford.

1674.4[s] and ends at 2080.4[s]. It skipped the 1674.4 seconds of dynamic calculation and tried to capture the response of that maximum wave height that occurred at 2074.4[s]. The result of the short simulation will be slightly unique value. The transient solution is responsible for the difference. The 406 seconds simulation produced an acceptable result with less than 1% difference in all three cases; the 606 seconds simulation produce a better result at the price of 30% more computational afford.
The differences become smaller with longer simulation time. Namely, 806-seconds simulations gives a result that almost zero difference. The result of the 206-seconds and 306-seconds simulations seems not bad in this three simulation. But it can be unstable with more simulations. Therefore, the further study carried with 406s and 606s simulations.

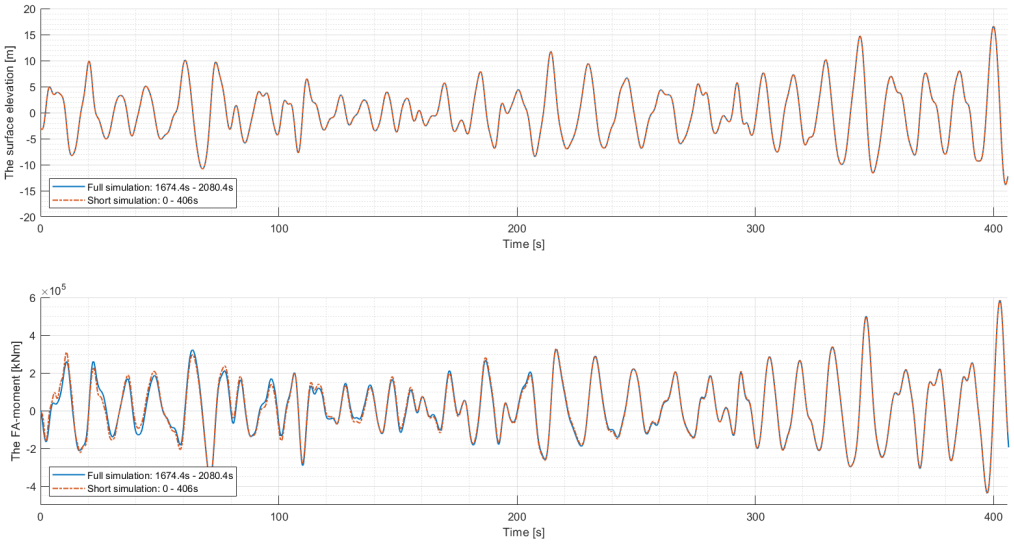

Figure 6.2: Comparing the time series of 1-hour simulation and short simulation - Surface elevation vs FA-moment

In the short simulation, the surface elevation is generated for 4000[s] as a 1-hour simulation, but the dynamic calculation is carried on parts of it. If the timing is correct than the surface elevations should be on top of each other. The transient effects in the FA-moment is observable in the beginning and become smaller towards the end. The two time series seems to be identical after 300 seconds, but there is a slight difference if one zooms inn.

The Figure 6.2 comparing the 406 seconds short simulation time serie with relative interval of the 1-hour simulation time serie. The interval starts from 400 seconds before the maximum wave height and continuous 406 seconds.The time series are taken from the simulation with seed=200. As a reminder, the short simulation using relative parts of the full 1-hour surface elevation time series; the two surface elevations should be exactly matched, if the timing is correct. The time series of the FA-moments are converges to each other as time goes; the dynamic calculation is finding its equilibrium position. The difference becomes not observable from the figures after 300s.

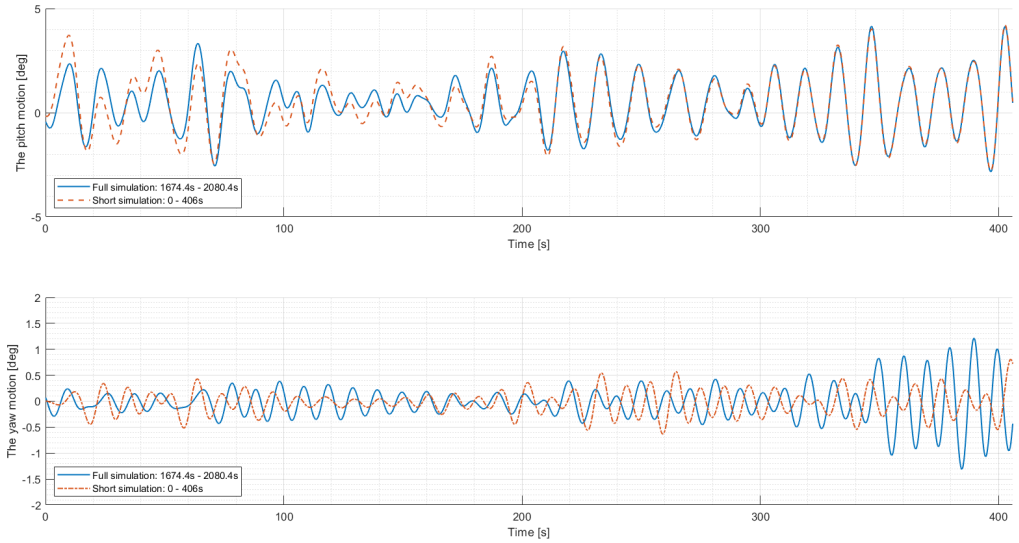

Figure 6.3: Comparing the time series of 1-hour simulation and short simulation - Pitch vs Yaw

The transient effects in the pitch motion similar to transients in FA-moment. It is on a reasonable level in 300 to 400 seconds. The transients of the Yaw motion have not disappeared in 400 seconds.

The Figure 6.3 visualizes the transient effects in the pitch and yaw motions. The relative interval of the full 1-hour simulation time series is plotted together with 406-seconds short simulation time series. The pitch motion presents a slightly larger difference in the beginning. But the major trend is almost same as FA-moment and the time series seems converged after 300s. The yaw motion is not converging at all in even 400s seconds; further investigation is needed.

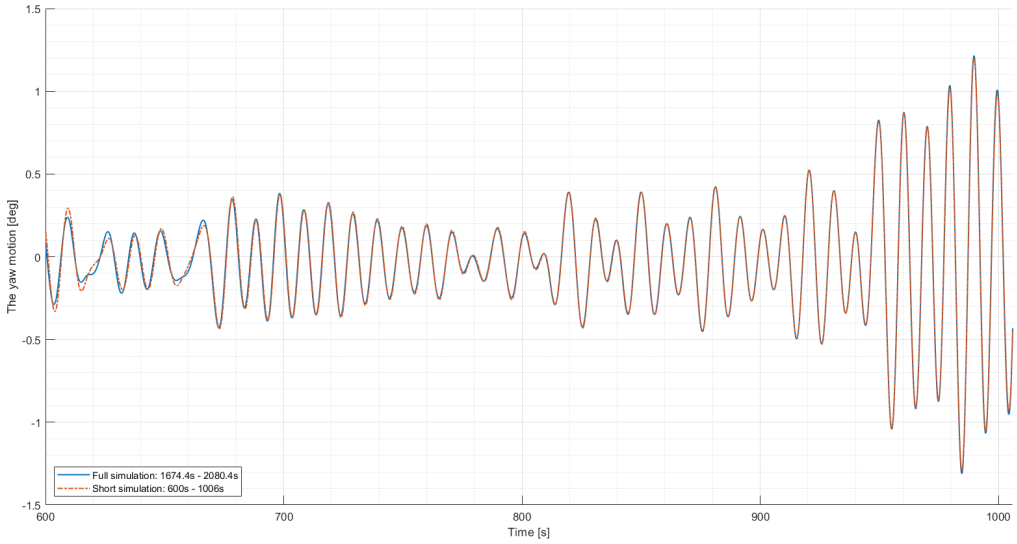

Figure 6.4: Comparing the time series of 1-hour simulation and short simulation - Yaw

The 1006-seconds short simulation time series compared with the relative parts of the full 1-hour simulation time series. The aim is to investigating how long pre-simulation is needed for yaw motion for a proper initialization. The transient effect seems small in 700 to 800-seconds on current plot.

In order to investigate how long the transient effect exists in Yaw motion, a 1006-seconds short simulation time series is plotted together with the corresponding part of the full 1-hour simulation in Figure 6.4. The transient effect seems small in 700 to 800-seconds on current plot, but a 806-seconds short simulation results a significant difference in yaw motion at maximum wave height. It may be because the yaw motion is slight in our model and tiny difference can have a significant impact on the percent calculation. However, the transients of the yaw motion is not important in our case; the yaw motion is slight. We are suggesting to have a further investigation on initialization period, in case the yaw motion is significant.
Based on results in Figure 6.1, we decided to further investigate the 406-seconds and 606-seconds short simulations with 100 seeds. In other words, the six-seconds interval which starts at the index of maximum wave height is the major purpose. Two pre-simulation lengths are applied; they are 400-seconds and 600-seconds.
The results of the short simulations compared with the reference. The reference is the response of maximum wave height in 1-hour simulation. Specifically, the reference is the maximum FA-moment in the six-seconds interval which starts at the index of maximum wave height. As a reminder, if the pre-simulation in short simulation is long enough, the results should be identical. In our case, however, the 400-seconds and 600-seconds simulations expected to introduce a slight difference.

In addition, to run 606 seconds approach in some simulations is not practically convenient. For example, with seed 109 the maximum wave height appears at 503.6[s] on the 4000 seconds time interval. Here, the simulation starts at -96.4[s] which is difficult to apply. Therefore, the results of 606 seconds approach does not include the 10 such seeds.
The results are presented in the Figure 6.5. The 606 seconds approach resulted in less error as expected; the differences are close to zero in 99 simulations. However, the difference with 406-seconds short simulation in an acceptable level; 98 simulations introduced an error less than $\pm 1.5\%$. There is only one exceptional point that behaves differently in both simulations.

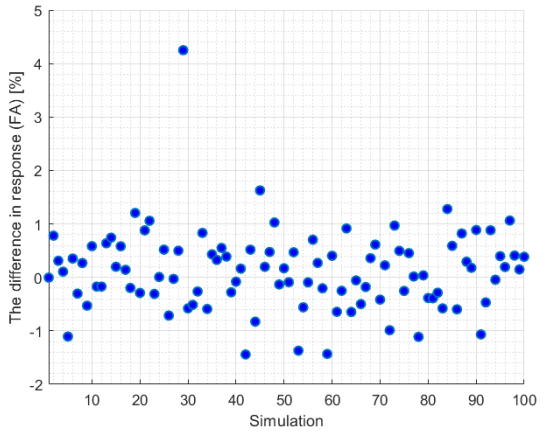

(a) 406-seconds simulation

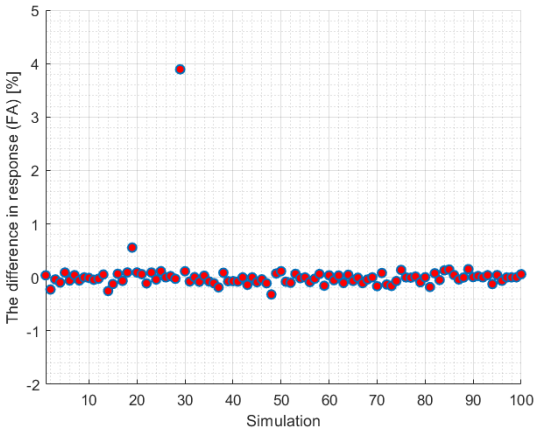

(b) 606-seconds simulation

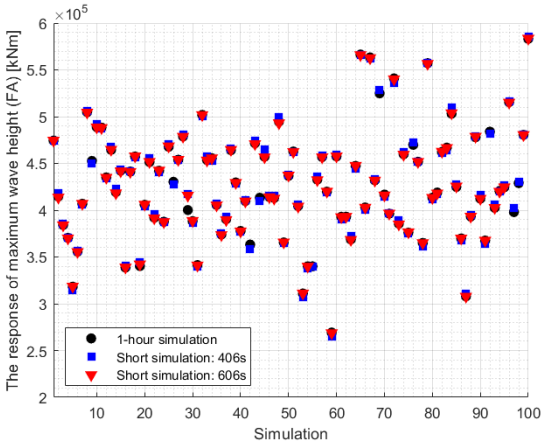

(c) The response of maximum wave height

Figure 6.5: Comparing the results of short simulations with maximum wave height responses of 1-hour simulation

The reference is the response of maximum wave height in full 1-hour simulation; each seed has a reference. The short simulations carried in 406-seconds and 606-seconds with 100 seeds. The 606 seconds approach resulted in less error as expected, but the difference with 406 seconds approach is in an acceptable range.

The simulation with seed=129 introduces a difference of 4% in both simulations. Interestingly, there is no significant decrease in the error with longer simulation time. The difference in varied simulation length are presented in plot(c) in Figure 6.6. Diving into the time series shows that a strange oscillation in the time series is responsible for the difference. The oscillation starts about 10 seconds before the maximum wave height and lasts about 80 second. It presented in plot(a) in Figure 6.6. Further study is required to understand more about the problem. However, it is one case out of 100 and the introduced 4% is not significant comparing to total uncertainty in the estimation. 400-seconds initialization time works for our purpose.

The Figure 6.7 is comparing the results of 406-seconds simulations at $1^{st}/2^{nd}$ maximum wave height with reference. The reference is the response of $1^{st}/2^{nd}$ maximum wave height in the 1-hour simulation. The larges difference is 1.6%. The special case behaves normal in this time. The response of the second maximum wave height is larger in the simulation with seed=129; the short simulation, therefore, carried at the second maximum wave height. Thus, the oscillation is not presented. The major purpose of a short simulation at wave height is saving time when predicting the response of maximum wave height. The Figure 6.8 shows the distributions of the short simulations compared with the reference distributions. The result distributions of the 406-seconds and 606-seconds short simulations at maximum wave height compared with the response distribution of maximum wave height in 1-hour simulation. Similarly, the result distributions of the 406-seconds short simulations

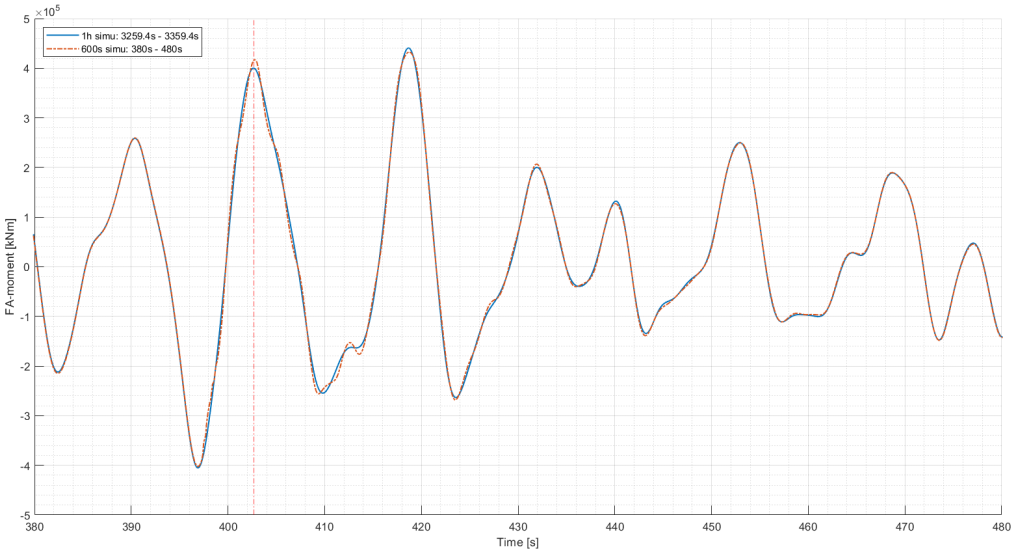

(a) Time series of a 406-seconds simulation

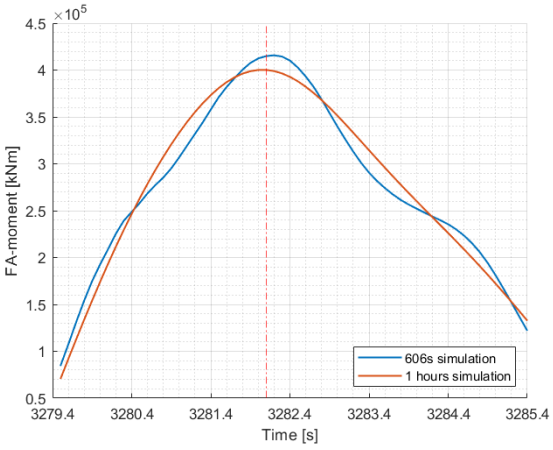

(b) Zooming to the maximum wave height response in 606-seconds simulation

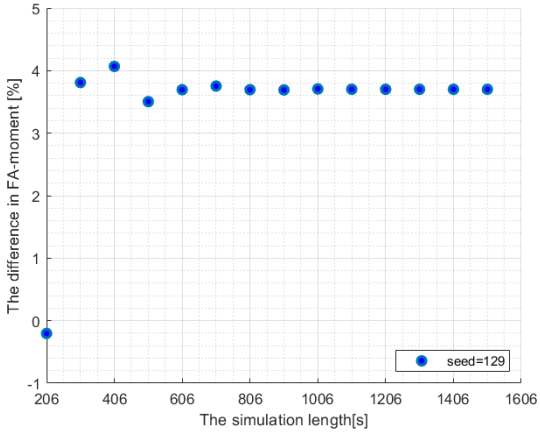

(c) Comparing the difference with varied simulation length

Figure 6.6: A further study on the speacial case: simulation with seed 129

The short simulation approach with seed 129 results slighly larger difference. Interestingly, there is no significant decrease in the error with longer simulation time. A strange oscillation in the time series is responsible for this. It starts before the maximum wave height and lasts about 80 second.

at $1^{st}/2^{nd}$ maximum wave height compared with the response distribution of $1^{st}/2^{nd}$ maximum wave height in 1-hour simulation. The sample distributions are almost same with slight differences. The variations are negligible. The results of the short simulations then fitted to Gumbel distribution and compared with reference Gumbel distribution Figure 6.9. The fitted result distributions of short simulations seem identical to the reference.

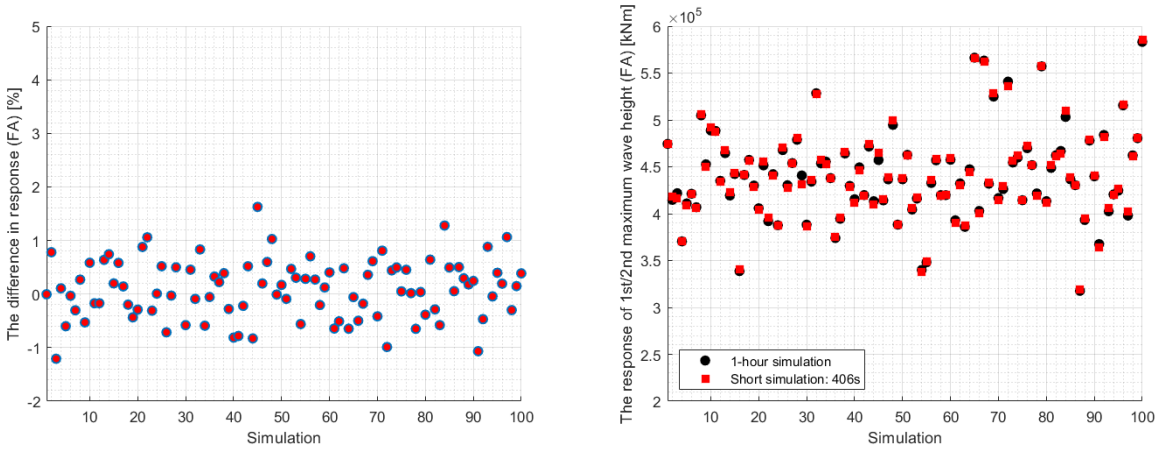

(a) The difference (b) The actual values

Figure 6.7: Comparing the results of 406-seconds simulations at $1^{st}/2^{nd}$ maximum wave height with response of $1^{st}/2^{nd}$ maximum wave height in 1-hour simulation

The response of $1^{st}/2^{nd}$ maximum wave height in the 1-hour simulation. The result of the short simulation is the maximum FA-moment in the two six-seconds intervals after the 1st/2nd maximum wave height. The difference is on an acceptable level.

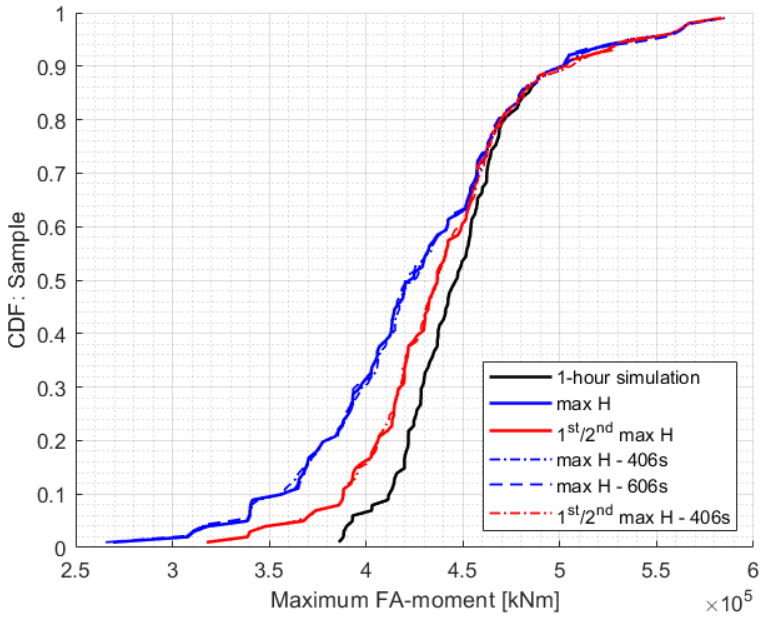

Figure 6.8: Comparing the results of short simulation approaches with the references in CDF

When considering the response of maximum wave height, both results of 406-seconds and 606-seconds seem to follow the reference distribution well. The plot is only for a visual comparison, and a more detailed comparison comes on the table.

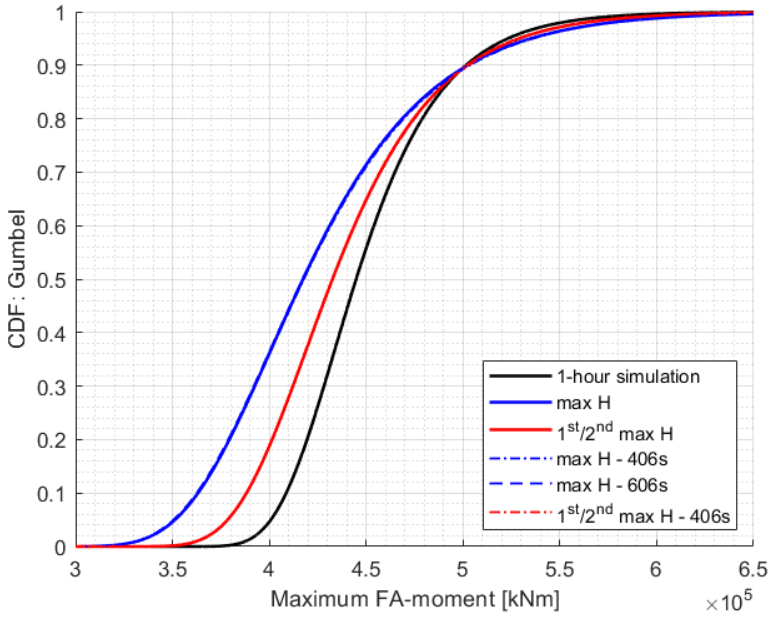

Figure 6.9: Comparing the results of short simulation approaches with the references in Gumbel distribution

The fitted distributions seem almost identical and 406-seconds simulation seems to work with its purpose. Further details comes in the table.

6.3 Summary

Based on the results in phase I, the response of maximum wave heights can be found by a six-seconds simulation with proper initialization time. In the time series that we studied, the surge, pitch and FA-moments reach their equilibrium state approximately in 400 seconds Figure 6.2, Figure 6.3. While yaw motion needs a minimum 800 seconds Figure 6.4.

The six-seconds simulation with 400-seconds initialization gives a result varied less than 1.6% from maximum response of full simulation in 99% cases. The six seconds simulation with 600-seconds initialization gives a more accurate result Figure 6.5. In both cases, the sample distributions and the fitted Gumbel models are not presented any significant difference comparing to the 1-hour simulation result Figure 6.8,Figure 6.9.

The 400-seconds initialization time produce a decent result in case the second maximum wave height is included. It presents less than 1.6% difference in all 100 cases compare to 1-hour simulation Figure 6.7.

Chapter 7

Phase-III

7.1 method

In standards, the USL control for design of FOWT structure defined as the 98% quantile in the distribution of the annual maximum combined load/load effect [4]. It corresponds to the combined load effect that has 50 years return period. In principle, the distribution of the annual maximum load effect is obtained by a long-term response analysis, which considering all the environmental states. However, the design standards allowed to estimate the characteristic response using the contour line approach. The expected value of the maximum response in the worst environmental state that has a 50 years return period applied as characteristic response [6]. Further, minimum total 5-hours simulation is required for characteristic response estimation [6]. Therefore, a characteristic response is estimated by means of five 1-hour simulations generated maximum responses.
The studies in phase-I show that the expected value of the response of maximum wave height in 1-hour simulation is a reasonable approximation to the expected value of the maximum response. The presented difference was about 5%. If including the response of the second maximum wave height, the difference reduced to about 2%. Further, the results in phase-II show that the six seconds simulation with 400-seconds initialization worked well to determining the responses of the maximum wave heights.
Based on the results, the characteristic response can be estimated by the results of short simulations. How large the combined uncertainty is, if the characteristic response estimated with the short-simulation approach? Is the short-simulation approach applicable in the practical design process? How about the variation of the result? In this phase, we are applying short-simulation approach for characteristic response estimation and comparing the results with full 1-hour simulation result.
The characteristic responses estimated by various approaches listed on the table and plotted as sample distribution appendix B,Table 7.1. The number of characteristic responses in each approach is limited. Therefore, the characteristic responses are fitted to an existing probability model for a smooth distribution. The Gumbel model is used after some trials on probability paper with varied models. To have a good visual impression to the variations of the characteristic values in each approach, they compared in the PDF distribution Figure 7.4.
Assume, the alternative statistical method for characteristic response estimation is using the largest response in five 1-hour simulations. Then the short-simulation approach expected to work better. Because the largest of the maximums corrosponds to a higher quantile in the maximum response distribution. The critical maximum response in the 1-hour simulation is more probability relate to maximum wave height. Therefore, the response distribution of maximum wave height converges to the maximum response distribution Figure 5.6.
We tested the applicability of the method as an alternative approach.

7.2 Result

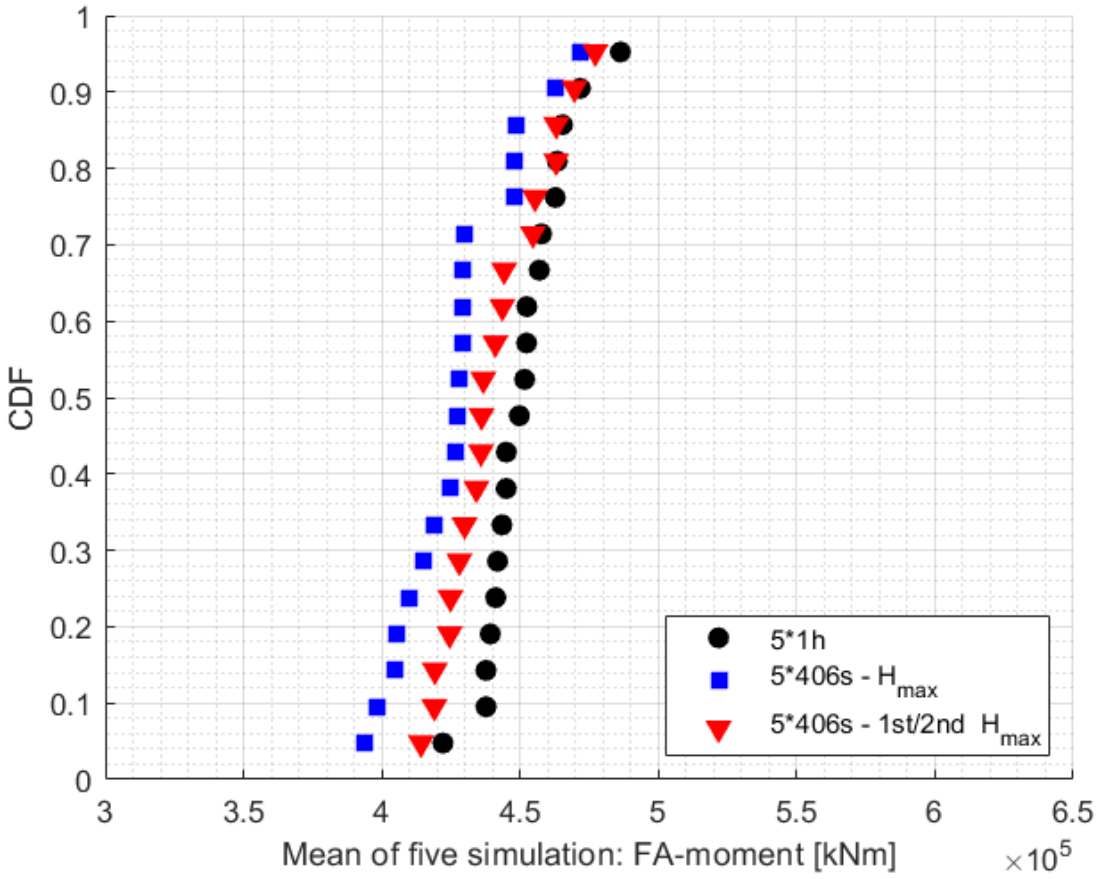

Figure 7.1: The characteristic value distributions: Mean of five maximums

*5*1h = the characteristic response estimated with 1-hour simulations.*
*5*406s H_{max} = the characteristic response estimated with short-simulation approach where considered only the response of maximum wave height.*
*5*406s - 1st/2nd H_{max} = the characteristic response estimated with short-simulation approach; including the response of second maximum wave height.*

Based on the design rules, the characteristic value for ULS estimated by the mean value of five maximum response in the environmental state that has 50 years return period. The 100 maximum FA-moments of 1-hour simulations results 20 characteristic values. The distribution of them is a reference to the applicability of the short simulation approaches in the characteristic value estimation. When considering only the response of maximum wave height, the difference in characteristic value less than 10.4%. Including the response of 2^{nd} maximum wave height in considering the difference in characteristic reduced to 6.1% Table 7.1.

20-40 samples is required to have a reasonable fit to Gumbel model when using the method of moments [13]. The sample size in this case is 20. The fitted model seems reasonable for our purpose. The deviations of the sample from the fitted model is less than 2% Figure C.2. The histograms of reference and approach-II behave more or less similarly. They are not symmetrical as a normal distribution witch usually works well to the mean value problems. The approach-I is less steep on the left-hand side, but still seems to have a long tail on the right-hand side.However, it should be in mind that 20 samples are little in order to describe a distribution behavior in histogram Figure C.1.

The expected value of approach-I is 5.3% less than reference; the expected value of approach-II

Seeds	S_K[kNm]	S_K-I [kNm]	D-I [%]	S_K-II [kNm]	D-II [%]
101,121,141,161,181	443431	429606	3.1	443579	0
102,122,142,162,182	437672	405026	7.5	424814	2.9
103,123,143,163,183	437677	427297	2.4	436702	0.2
104,124,144,164,184	452343	424525	6.1	424525	6.1
105,125,145,165,185	471769	448612	4.9	469649	0.4
106,126,146,166,186	439208	393552	10.4	418995	4.6
107,127,147,167,187	457765	429430	6.2	436045	4.7
108,128,148,168,188	462693	463045	-0.1	463045	-0.1
109,129,149,169,189	456928	447883	2	455397	0.3
110,130,150,170,190	452436	429213	5.1	434194	4
111,131,151,171,191	449723	410035	8.8	435846	3.1
112,132,152,172,192	486251	471664	3	477160	1.9
113,133,153,173,193	441179	405440	8.1	441011	0
114,134,154,174,194	444975	419184	5.8	419184	5.8
115,135,155,175,195	422092	398326	5.6	414161	1.9
116,136,156,176,196	451623	428036	5.2	428036	5.2
117,137,157,177,197	441855	429336	2.8	429921	2.7
118,138,158,178,198	445025	426597	4.1	444209	0.2
119,139,159,179,199	463420	415364	10.4	463093	0.1
120,140,160,180,200	465333	447738	3.8	454648	2.3

S_K = the characteristic response estimated with 1-hour simulation; as a reference
S_K-I = the characteristic response estimated with short-simulation where considered only the response of maximum wave height
D-I= the difference between the S_K and S_K-I
S_K-II = the characteristic response estimated with short simulation where the response of second maximum wave height is included.
$D_I I$ = the difference between the S_K and S_K-I

Table 7.1: Comparing the characteristic responses which estimated with various approaches

is 2.3% less than reference. However, the characteristic response distribution generated by short-simulation approaches has a wider band. Which refers to that the estimated characteristic responses using a short simulation approach varies larger than 1-hour simulation results. The variation not expected to reduce significantly by increasing the number of seeds in the simulation Figure 7.4.

Applying a 10% correction the estimated characteristic response based on short-simulation become 4.2% conservative in expected value comparing to the full simulation result. The 4.2% can be an excellent compromise to the wide variation. Despite of twice longer simulation, we prefer to include the response of the second maximum wave height, which only present 2.3% less in expected value of the characteristic response comparing to full simulation result. With 5% correction, the expected value of characteristic response become2.6% conservative. Maybe it is a suitable compromise to a wider variation band Figure 7.5.

If the characteristic response estimated by the maximum results of five seeds, then the short-simulation approach works better considering only the maximum wave height. The short-simulation introduces a difference less than 1.3% in 19 characteristic responses comparing to the results of full 1-hour simulation. One exception presents a 8.8% difference. There is no significant improvement including the second maximum wave height response into consideration Table 7.2 . The variation expected to be sensitive to the number of seeds used. Applying the approach with existing load factors is too conservative.

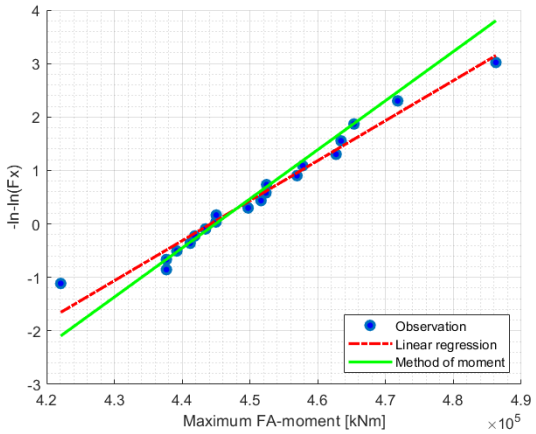

(a) Reference characteristic value

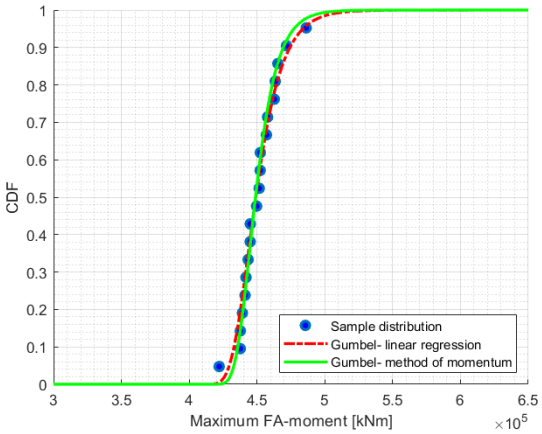

(b) Reference characteristic value

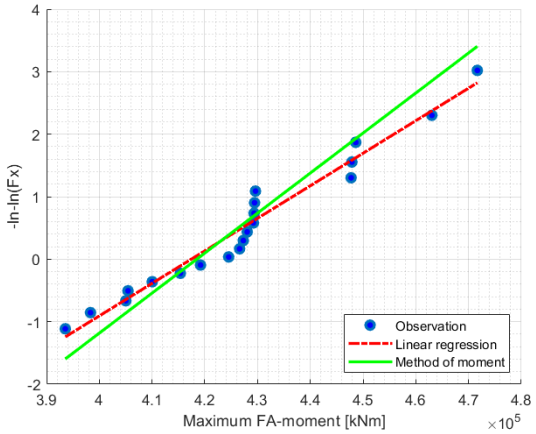

(c) The short simulation approach I

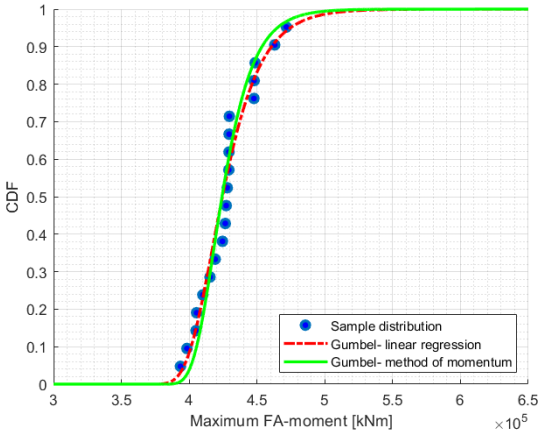

(d) The short simulation approach I

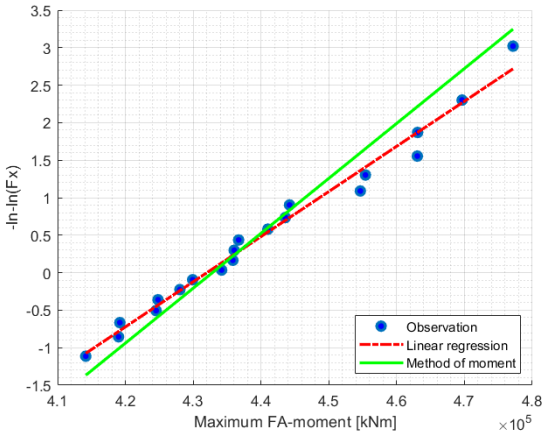

(e) The short simulation approach II

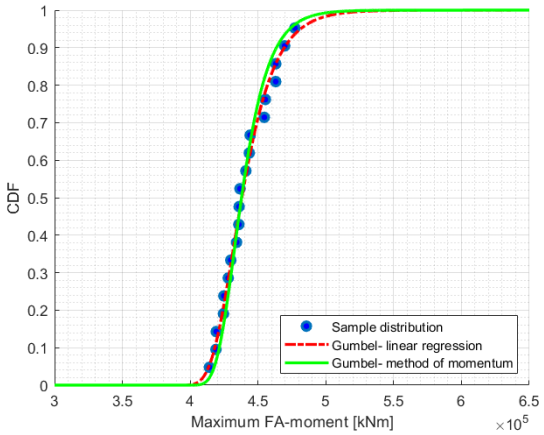

(f) The short simulation approach II

Figure 7.2: Testing the fitted gumbel model in probabilty paper

Reference: the characteristic response generated by 1-hour simulations.
Approach-I: the characteristic response estimated by short-simulation.
approach at maximum wave height.
Approach-II: the characteristic response estimated by short-simulation approach, including the response of second maximum wave height.

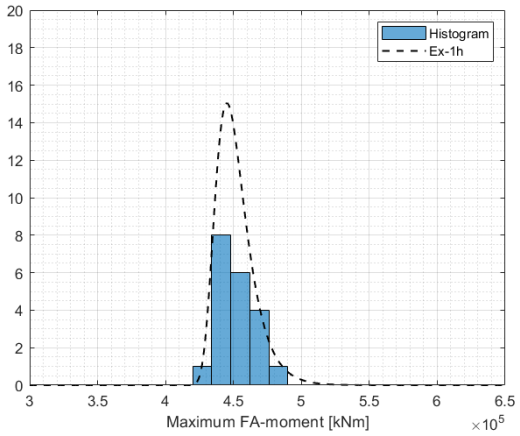

(a) Reference characteristic value

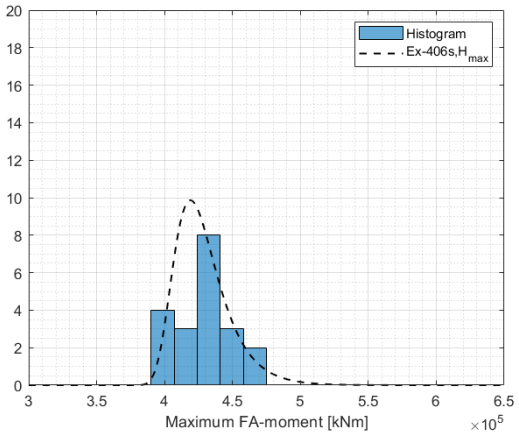

(b) The short simulation approach I

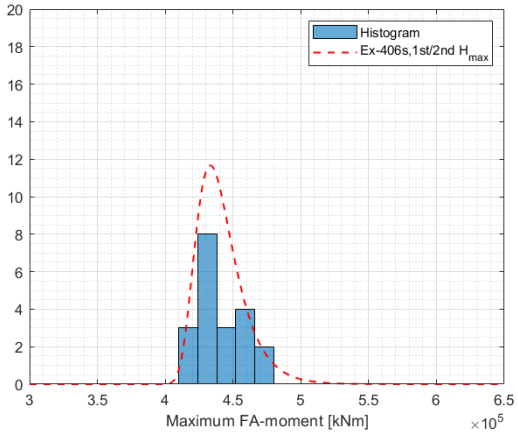

(c) The short simulation approach II

Figure 7.3: Histogram vs PDF (fitted Gumbel model)

Reference: the characteristic response generated by 1-hour simulations.
Approach-I: the characteristic response estimated by short-simulation.
approach at maximum wave height.
Approach-II: the characteristic response estimated by short-simulation.
approach, including the response of second wave height.

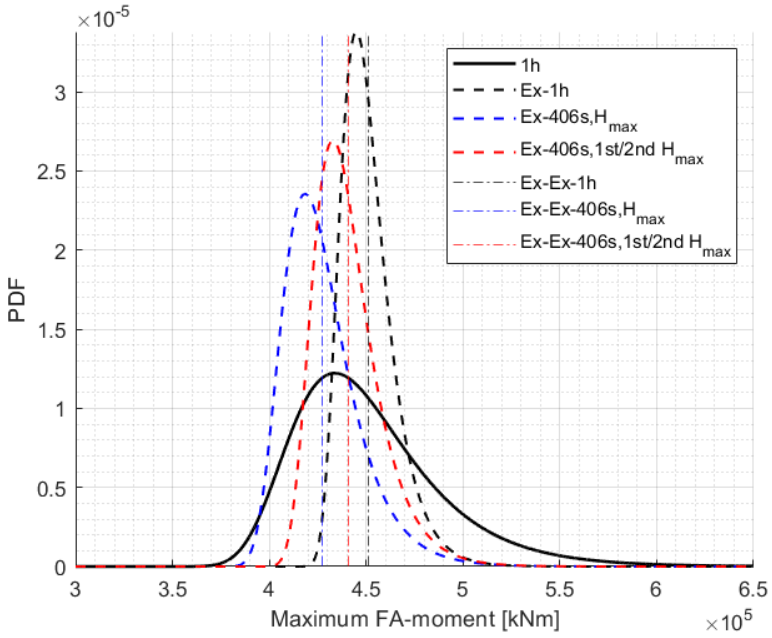

Figure 7.4: The characteristic response distributions

Reference: Ex-1h; the characteristic response generated by 1-hour simulations.
Approach-I: Ex-(406s,H_{max}); the characteristic response estimated by short-simulation approach at maximum wave height.
Approach-II: Ex-(406s,$1^st/2^nd$ H_{max}); the characteristic response estimated by short-simulation approach, including the response of second wave height.

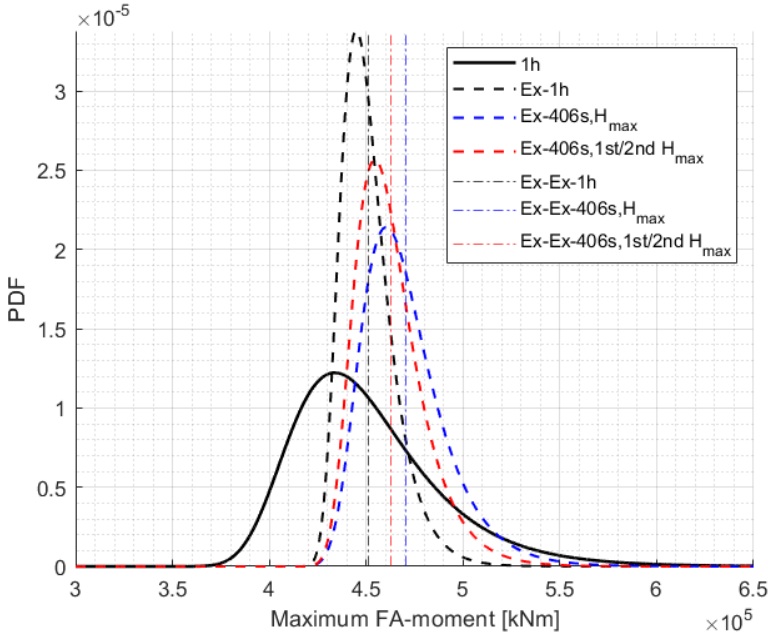

Figure 7.5: The characteristic response distributions (Illustrating with corrections)

Ex-1h: Reference; the characteristic response generated by 1-hour simulations.
Ex-(406s,H_{max}): Approach-I with 10% correction; the characteristic response estimated by short-simulation approach at maximum wave height.
Ex-(406s,$1^st/2^nd$ H_{max}): Approach-II with 5% correction; the characteristic response estimated by short-simulation approach, including the response of second wave height.

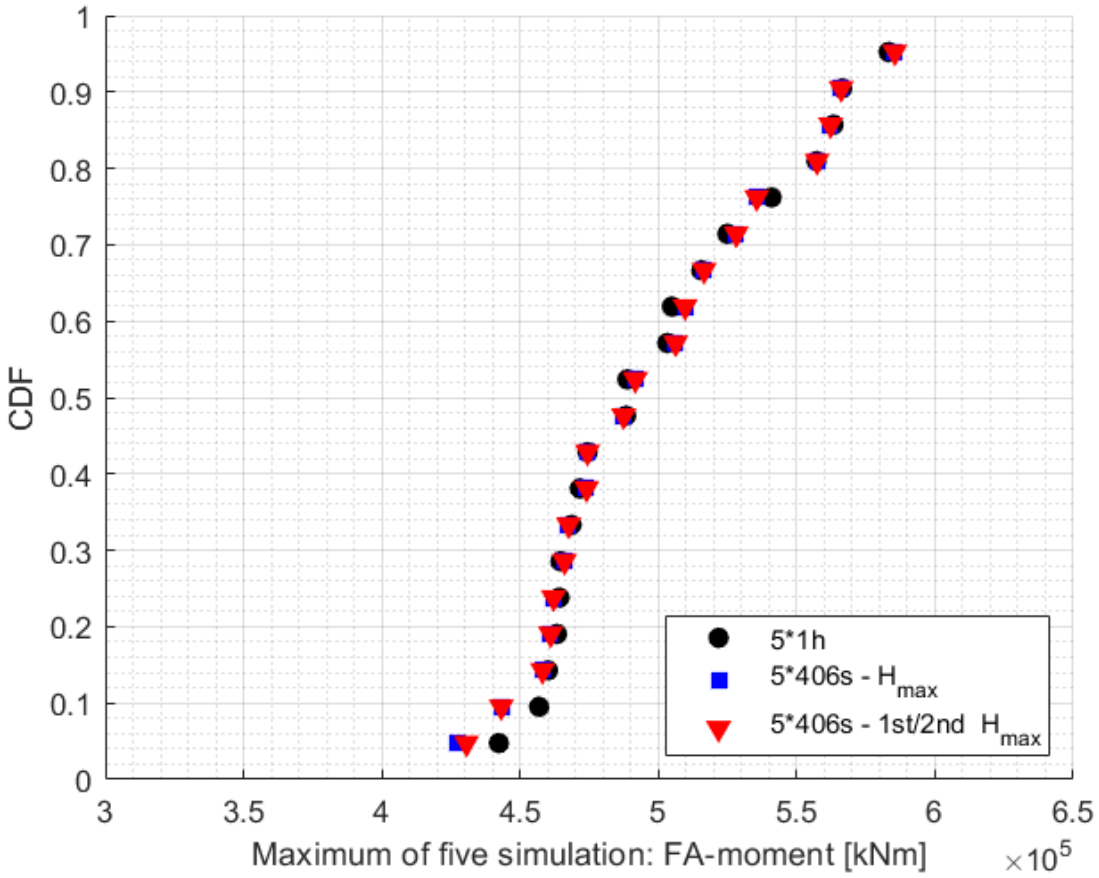

Figure 7.6: The characteristic value distributions: maximum of five maximums

*5*1h = the characteristic response estimated with 1-hour simulations.*
*5*406s H_{max} = the characteristic response estimated with short-simulation approach where considered only the response of maximum wave height.*
*5*406s - 1st/2$nd$$H_{max}$ = the characteristic response estimated with short-simulation approach; including the response of second maximum wave height.*

Seeds	S_K[kNm]	S_K-I [kNm]	D-I [%]	S_K-II [kNm]	D-II [%]
101,121,141,161,181	474397	474375	0	474375	0
102,122,142,162,182	463282	461021	0.5	461021	0.5
103,123,143,163,183	471583	474026	-0.5	474026	-0.5
104,124,144,164,184	503209	509642	-1.3	509642	-1.3
105,125,145,165,185	566397	566070	0.1	566070	0.1
106,126,146,166,186	468592	427292	8.8	430612	8.1
107,127,147,167,187	563261	562246	0.2	562246	0.2
108,128,148,168,188	504868	506224	-0.3	506224	-0.3
109,129,149,169,189	524917	528135	-0.6	528135	-0.6
110,130,150,170,190	488785	491640	-0.6	491640	-0.6
111,131,151,171,191	488265	487422	0.2	487422	0.2
112,132,152,172,192	540898	535547	1	535547	1
113,133,153,173,193	464581	467545	-0.6	467545	-0.6
114,134,154,174,194	460063	462082	-0.4	462082	-0.4
115,135,155,175,195	442319	443198	-0.2	443198	-0.2
116,136,156,176,196	515517	516515	-0.2	516515	-0.2
117,137,157,177,197	456869	458107	-0.3	458107	-0.3
118,138,158,178,198	464227	466035	-0.4	466035	-0.4
119,139,159,179,199	557141	557352	0	557352	0
120,140,160,180,200	583208	585458	-0.4	585458	-0.4

S_K = the characteristic response; the maximum of five 1-hour simulation results; the reference
S_K-I = the maximum of five results of 406-seconds simulation at maximum wave height.
D-I= the difference between S_K and S_K-I
S_K-II = the maximum of five results of 406-seconds simulation at wave height and second maximum wave height.
$D_I I$ the difference between S_K and S_K-II

Table 7.2: The characteristic responses estimated with largest of five maximums

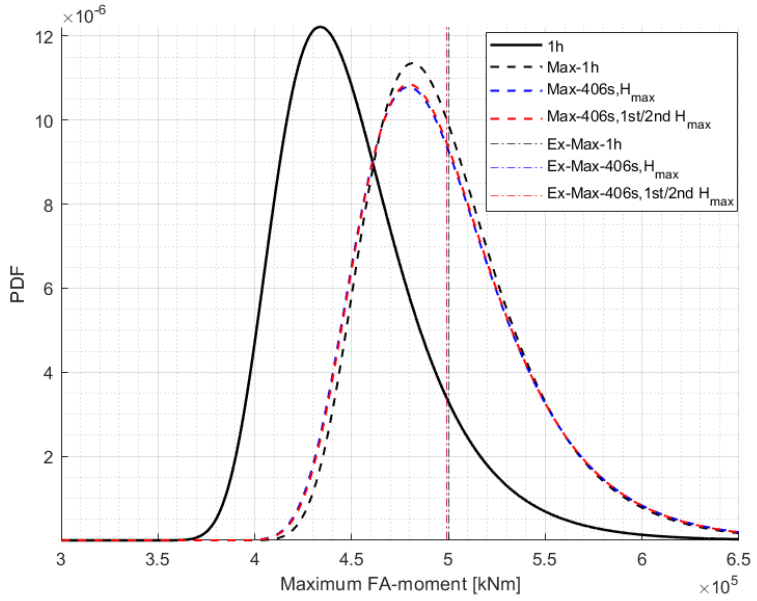

Figure 7.7: The characteristic response distributions (maximum of five maximums)

Max-1h: Reference; maximum value of five maximum FA-moment generated by 1-hour simulations.
Max-(406s,H_{max}): maximum value of five results of short-simulation at maximum wave height.
Ex-(406s,$1^s t/2^n d$ H_{max}): maximum of five results from short-simulation including the response of seond maximum wave height.

7.3 Summary

The estimated characteristic value based on the maximum wave height response in short-simulation approach introduced a difference less than 10.4% in 20 values that considered. Including the response of the second maximum wave height into account, the difference reduced to less than 6.1% Table 7.1. Including the response of second maximum wave height gives a better result.
The expected value of the fitted Gumbel distribution of characteristic response with short-simulation approach at wave height is 5.3% less than the expected value of the full simulation characteristic response distribution. Including the response of second maximum wave height, the difference in expected value reduced to 2.3% Figure 7.4. However, the characteristic response distributions got by the short-simulation approaches have wider variation than 1-hour simulation characteristic response distribution. The largest variations presented with considering only the response of maximum wave height.
If considering the largest response of five 1-hour simulation as a statistical method to characteristic response estimation, then the short-simulation approach works betterFigure 7.6. Because the maximums of five refers to higher quantile in the maximum response distribution. Considering only the maximum wave height response with short-simulation introduces a difference less than 1.3% in 19 characteristic responses Table 7.2. One exception presents a 8.8% difference. There is no significant improvement including the second maximum wave height response into consideration. However, the variation of the characteristic responses are wide and the characteristic response estimated with this method probably too conservative to apply with load factor. The variation is believed to be sensitive to the number of seeds, and the largest of ten responses would give a significant less variation. However, an additional study needed to combine this approach with load factor.

Chapter 8

Conclusion

8.1 The short-simulation approach in SIMA

The current study suggesting and validating a short-simulation approach for ULS characteristic response estimation for tower base bending moment on a critical load case DLC_6.1. This approach may also be applicable to other design drivers where the wave expected to be dominant. This approach can be applied in SIMA in two ways. The first one is combining the Matlab/Python with SIMA. The specific steps can be:

- Step 1: generate the surface elevation in matlab/python.
- Step 2: determine where the wave extremes occur; determine the index of wave extremes.
- Step 3: create a surface elevation import file to SIMA.
- Step 4: set the start time of dynamic calculation for 400 seconds before the maximum wave height index and run the simulation for 406 seconds.

The specific steps for another way can be:

- Step 1: set the requested time series length to 4000 seconds in the time series generation parameter settings.
- Step 2: set the dynamic calculation starting time towards the end of the time series and run a few seconds simulation witch ends at 4000[s]. Because it will not generate the wave after dynamic calculation ends.
- Step 3: determining where the wave extremes occure; determine the index of wave extremes.
- Step 4: rerun the simulation with same seed; start the dynamic calculation for 400 seconds before the maximum wave height index; run the simulation for 406-seconds.

The response of wave extremes is in the last six-seconds interval of the response time series.

8.2 Summary

Based on the results in Phase I, the maximum FA-moment is the dominant response at the tower base in DLC_6.1. Further, one can expect that the response of a specific wave height will happen in six seconds. The largest maximum responses are following the maximum wave height. Therefore, the maximum response distribution converges to the response of maximum wave height distribution in high quantile. It seems possible to estimate characteristic response with response of maximum wave heights using proper statistical methods. Considering the practicality, current study only considered the first and second maximum wave height. They responsible for 50% and 70% maximum responses in the full simulation. The expected values of the estimated characteristic response based

on wave height responses present 5.4% and 2.4% differences comparing to the full 1-hour simulation based characteristic response expected value. The results in phase II shows that it is reasonable to assume that 400-seconds initialization time is proper to our purpose. Therefore, the response of maximum wave heights can be predicted with six-seconds simulation with 400-seconds initialization time. The 600-seconds initialization can be applied for more precise result with increased simulation time. However, 400-seconds initialization time and including the response of the second maximum wave height will produce a much better approximation of the maximum response in full 1-hour simulation.
Using the results from phase I and phase II, we suggested a short-simulation approach to estimating the characteristic response for design purpose. The characteristic response estimated by short-simulation approach at the maximum wave height present 5.3% less in expected value than full 1-hour simulation results. In addition, the variation of the characteristic response based on short-simulation approach is slightly wider. Applying 10% correction the estimated characteristic response based on short-simulation become 4.2% conservative in expected value comparing to the full simulation result. The 4.2% can be an excellent compromise to the wide variation.
Despite of twice longer simulation, we prefer to include the response of the second maximum wave height, which only present 2.3% less in expected value of the characteristic response comparing to full simulation result. With 5% correction, the expected value of characteristic response become 2.6% conservative. Maybe it is a suitable compromise to a wider variation band.
If the characteristic response estimated by the maximum results of five seeds, then the short-simulation approach works better considering only the maximum wave height. We suggested it as an additional approach for characteristic value estimation. It is promising to work with a proper number of seeds. However, a further study should be carried to find a statistically proper method to combine with the design load factors. Because applying the approach with existing load factors is tent to be too conservative.

8.3 The advantages of the suggested short-simulation approach

- Frist, the short-simulation approaches will reduce simulation time. For example, the 100 1-hour simulations carried about 17 hours on a modern PC. The 100 406-seconds simulation, on the other hand, were simulated in 3 hours on the same PC. The short simulation approach is about six times more effective than 1-hour simulation in this specific case.

- Second, the short simulation approaches generates small size of data. Continue with previous example, the 100 1-hour simulation took a 8.50[GB] storage space while the 100 406-seconds simulation took a 2.64[GB] storage space. In a rough estimation, the short simulation was three times more storage effective than the 1-hour simulation.

- Third, the short simulation approaches cen be applied in longer simulation than 1-hour. Because of the floating wind turbines have longer natural periods, it requires running longer simulation than the fixed ones. The 1-hour simulation allowed to apply in initial sizing and conceptional design process, but the design rule suggests running a minimum three hours simulation in wave loads dominated load cases [4]. The advantages in simulation time and storage space would be more obvious if the 3-hours simulation is applied.

8.4 Recommendation to further work

- Frist, the study mainly focused on the decay of the response, the initialization period and the relations between maximum response and response of the maximum wave height. To simplifying the investigation and properly understand the contributions from varous load processes, some environmental parameters are not included. However, they can have a significant effect

to the result. Namely, proper investigation of the current is important because the extreme current may introduce a high pitch angle. Especially when the wave and current is coming in the opposite directions. Such an acute pitch angle can introduce extra tower base banding moment at the tower base because of the gravitation force. In addition, the spar has a slight yaw stiffness and the validating with turbulence wind and misalignment is needed. Therefore, a further investigation on the effects of the neglected parameters to suggested approaches is important.

- Next, the suggested approaches should be validated in varous environmental conditions as well.
  To testing the applicability of the short-simulation approaches to estimating characteristic tension in the mooring line can also be interesting.

- The suggested short-simulation approach can also work for other design load cases which the wave loads expected to be the dominant environmental load. For example, the applicability to the design load case DLC_6.2 can be investigated.
  The suggested additional approach which using the largest response at maximum wave height in several short-simulations seems promising to produce a decent result in a significant reduced simulation time. However, a further investigation is needed to validate this approach. Combining this approach with load factor can be too conservative.

Bibliography

[1] D G Caglayan et al. "The techno-economic potential of offshore wind energy with optimized future turbine designs in Europe". In: *Applied Energy* 255 (2019). ISSN: 03062619.

[2] M Collu and M Borg. "11 - Design of floating offshore wind turbines". In: *Offshore Wind Farms*. 2016, pp. 359–385. ISBN: 978-0-08-100779-2.

[3] DNV.GL. *DNVGL-RP-0286: Coupled analysis of floating wind turbines*. Tech. rep. 0. URL: http://www.dnvgl.com.

[4] DNV.GL. *DNVGL-ST-0119: Floating wind turbine structures*. Tech. rep. 2018. URL: http://www.dnvgl.com.

[5] DNV.GL. *DNVGL-ST-0126: Support structures for wind turbines*. Tech. rep. 2016. URL: http://www.dnvgl.com.

[6] DNV.GL. *DNVGL-ST-0437: Loads and site conditions for wind turbines*. Tech. rep. 2016. URL: http://www.dnvgl.com.

[7] John D Fenton. "A Fifth-Order Stokes Theory for Steady Waves". In: *Journal of Waterway, Port, Coastal, and Ocean Engineering* 111.2 (1985), pp. 216–234. ISSN: 0733-950X.

[8] Sverre Haver, Kåre Edvardsen, and Gunnar Lian. "Uncertainties in Wave Loads on Slender Pile Structures Due to Uncertainties in Modelling Waves and Associated Kinematics". In: *The Proceedings of the ... International Offshore and Polar Engineering Conference*. Vol. 3. Cupertino: International Society of Offshore & Polar Engineers, 2017, p. 104. URL: http://search.proquest.com/docview/2137114664/.

[9] John Marius Hegseth and Erin E Bachynski. "A semi-analytical frequency domain model for efficient design evaluation of spar floating wind turbines". In: *Marine Structures* 64 (2019), pp. 186–210. ISSN: 0951-8339.

[10] Lin Li, Zhen Gao, and Torgeir Moan. "Joint distribution of environmental condition at five European offshore sites for design of combined wind and wave energy devices.(Report)(Author abstract)". In: 137.3 (2015), p. 31901. ISSN: 0892-7219.

[11] NEK. *NEK IEC 61400-3-1: Design requirements for fixed offshore wind turbines*. Tech. rep. 2019.

[12] NEK. *NEK IEC TS 61400-3-2: Design requirements for floating offshore wind turbines*. Tech. rep. 2019.

[13] Sverre Haver. "Metocean Modelling". In: *Metocean modelling and prediction of extremes*. Draft vers. Stavanger, 2019. Chap. Chapter 8, pp. 89–120.

[14] Joey Velarde and Erin E Bachynski. "Design and fatigue analysis of monopile foundations to support the DTU 10 MW offshore wind turbine". In: *Energy Procedia* 137.C (2017), pp. 3–13. ISSN: 1876-6102.

[15] K Wei et al. "Toward performance-based evaluation for offshore wind turbine jacket support structures". In: *Renewable Energy* 97 (2016), pp. 709–721. ISSN: 0960-1481.

Appendix A

The major results of 100 simulations

	Seeds	maxFA	FA_Hmax	sT406	$FA_4$06	FA_H1$H2max$	sT406H2	$FA_4$06$H2$
1	101	474400	474400	1682.1	474380	474400	1682.1	474380
2	102	414670	414670	1609.5	417910	414670	1609.5	417910
3	103	421840	384160	2392.1	385360	421840	2507.2	416750
4	104	388470	370440	239.1	370830	370440	239.1	370830
5	105	425750	318230	669.5	314710	410880	308.2	408420
6	106	441070	355710	2427.6	356960	421250	931.3	421110
7	107	414310	406870	2210.2	405630	406870	2210.2	405630
8	108	504870	504870	631.9	506220	504870	631.9	506220
9	109	452670	452670	103.6	450280	452670	103.6	450280
10	110	488780	488780	1434.1	491640	488780	1434.1	491640
11	111	488270	488270	1028.1	487420	488270	1028.1	487420
12	112	435030	435030	3011.2	434280	435030	3011.2	434280
13	113	464580	464580	632.7	467540	464580	632.7	467540
14	114	460060	419400	3338.7	422520	419400	3338.7	422520
15	115	442320	442320	2154.7	443200	442320	2154.7	443200
16	116	447140	338710	406.9	340680	338710	406.9	340680
17	117	454150	441320	1465.9	441950	441320	1465.9	441950
18	118	457350	457350	523.5	456440	457350	523.5	456440
19	119	430010	340320	2890.9	344420	430010	63.4	428140
20	120	428430	405800	3555.9	404620	405800	3555.9	404620

The units of FA-moment is [kNm]
Seeds = The seed
maxFA = maximum FA moment in 1-hour simulation
FA_Hmax = Response of maximum wave height
sT406 = The staring time for 406-seconds simulation
$FA_4$06 = The results of the 406-seconds short simulation at maximum wave height
FA_H1$H2max$ = The response of wave maximums; including first and second maximum wave height
sT406H2 The starting time considering the response of second maximum wave height
$FA_4$06$H2$ = The 406-seconds result including response of second maximum wave height

	Seeds	maxFA	FA_Hmax	sT406	$FA_4$06	$FA_H1H2max$	sT406H2	$FA_4$06$H2$
21	121	451520	451520	1453.8	455490	451520	1453.8	455490
22	122	428240	392020	1509.4	396170	392020	1509.4	396170
23	123	442160	442160	1519.6	440790	442160	1519.6	440790
24	124	437160	387680	2159.8	387710	387680	2159.8	387710
25	125	467830	467830	2559.8	470260	467830	2559.8	470260
26	126	453060	430370	184.3	427290	430370	184.3	427290
27	127	453950	453950	2018.3	453820	453950	2018.3	453820
28	128	478860	478860	1946.9	481250	478860	1946.9	481250
29	129	440790	400140	2879.4	417140	440790	2895.4	431490
30	130	428060	388290	2410.6	386040	388290	2410.6	386040
31	131	434180	341330	3132.8	339580	434180	154	436160
32	132	528470	501830	1755.9	500510	528470	1740.6	527990
33	133	453720	453720	1892.1	457490	453720	1892.1	457490
34	134	456120	455580	976.9	452890	455580	976.9	452890
35	135	437930	405690	1106.1	407440	437930	3312.1	437690
36	136	392880	374000	1315.4	375220	374000	1315.4	375220
37	137	424680	390390	1821.9	392540	394590	1835.3	395470
38	138	464230	464230	2769.4	466040	464230	2769.4	466040
39	139	429660	429660	1069.1	428460	429660	1069.1	428460
40	140	444130	377770	3244.7	377470	415400	314.9	412020
40	140	444130	377770	3244.7	377470	415400	314.9	412020
41	141	449460	409880	2430.8	410550	449420	3584.5	445910
42	142	419820	363250	124.6	358010	419820	902.3	418890
43	143	471580	471580	2046	474030	471580	2046	474030
44	144	485480	413370	154.6	409950	413370	154.6	409950
45	145	462140	457180	2823.9	464610	457180	2823.9	464610
46	146	468590	414220	2345.1	415040	414220	2345.1	415040
47	147	445620	413040	1323	415000	436610	109.8	439220
48	148	494730	494730	2464.7	499810	494730	2464.7	499810
49	149	388290	365520	3549.9	365030	388290	2363.3	388250
50	150	436720	436720	1205.1	437470	436720	1205.1	437470
51	151	462760	462760	3049.7	462350	462760	3049.7	462350
52	152	442910	404400	267.3	406300	404400	267.3	406300
53	153	421790	310950	2410.5	306690	416120	645.1	417390
54	154	428380	340010	1191.2	338100	340010	1191.2	338100
55	155	389890	340000	162.5	339680	348130	2659	349120
56	156	432730	432730	945	435780	432730	945	435780
57	157	456870	456870	3204.9	458110	456870	3204.9	458110
58	158	419770	419770	725.3	418910	419770	725.3	418910
59	159	419770	269200	869.4	265350	419770	2159.7	420280
60	160	457540	457540	302.5	459390	457540	302.5	459390
61	161	392930	392930	2370.4	390400	392930	2370.4	390400
62	162	463280	393000	2372.1	392010	432270	2359	430070
63	163	385930	368770	1391.5	372150	385930	1037.1	387790
64	164	447390	447390	2428	444500	447390	2428	444500

The units of FA-moment is [kNm]
Seeds = The seed
maxFA = maximum FA moment in 1-hour simulation
FA_Hmax = Response of maximum wave height
sT406 = The staring time for 406-seconds simulation
$FA_4$06 = The results of the 406-seconds short simulation at maximum wave height
$FA_H1H2max$ = The response of wave maximums; including first and second maximum wave height
sT406H2 The starting time considering the response of second maximum wave height
$FA_4$06$H2$ = The 406-seconds result including response of second maximum wave height

	Seeds	maxFA	FA_Hmax	sT406	$FA_4$06	$FA_H1H2max$	sT406H2	$FA_4$06$H2$
65	165	566400	566400	2363.6	566070	566400	2363.6	566070
66	166	402930	402930	638.3	400920	402930	638.3	400920
67	167	563260	563260	2115	562250	563260	2115	562250
68	168	431970	431970	743.2	433520	431970	743.2	433520
69	169	524920	524920	109.4	528140	524920	109.4	528140
70	170	468790	416660	2575.1	414930	416660	2575.1	414930
71	171	426210	396280	3533.6	397180	426210	3506.1	429660
72	172	540900	540900	3351.6	535550	540900	3351.6	535550
73	173	454540	385660	1586.3	389400	454540	435.8	456550
74	174	459800	459800	2171.5	462080	459800	2171.5	462080
75	175	415760	376030	2203.6	375070	414350	2217	414560
76	176	469850	469850	186.1	471980	469850	186.1	471980
77	177	451810	451810	3516.4	451880	451810	3516.4	451880
78	178	421570	364970	3586.8	360910	421570	1837.1	418830
79	179	557140	557140	2163.8	557350	557140	2163.8	557350
80	180	413360	413360	1032.7	411760	413360	1032.7	411760
81	181	448840	418850	1566.9	417220	448840	1738.4	451720
82	182	462350	462350	429.3	461020	462350	429.3	461020
83	183	466870	466870	3372.8	464160	466870	3372.8	464160
84	184	503210	503210	1830.1	509640	503210	1830.1	509640
85	185	436730	424900	1747.4	427410	436730	1870.6	438890
86	186	430380	369750	1970.5	367540	430380	830.8	430610
87	187	411690	307920	1586.5	310450	317710	2212.1	319310
88	188	403040	393270	2426.5	394420	393270	2426.5	394420
89	189	477970	477970	2559.6	478830	477970	2559.6	478830
90	190	439820	412340	2174.5	415990	439820	2633.8	440900
91	191	437190	367570	1681.3	363650	367570	1681.3	363650
92	192	483950	483950	49.9	481680	483950	49.9	481680
93	193	411260	402530	2565.9	406080	402530	2565.9	406080
94	194	420510	420510	2560.5	420330	420510	2560.5	420330
95	195	424560	424560	1727.8	426240	424560	1727.8	426240
96	196	515520	515520	1401.4	516510	515520	1401.4	516510
97	197	421770	397970	58.6	402210	397970	58.6	402210
98	198	462210	428930	106	430690	462210	1504.4	460830
99	199	480520	480520	271	481230	480520	271	481230
100	200	583210	583210	1674.4	585460	583210	1674.4	585460

The units of FA-moment is [kNm]
Seeds = The seed
maxFA = maximum FA moment in 1-hour simulation
FA_Hmax = Response of maximum wave height
sT406 = The staring time for 406-seconds simulation
$FA_4$06 = The results of the 406-seconds short simulation at maximum wave height
$FA_H1H2max$ = The response of wave maximums; including first and second maximum wave height
sT406H2 The starting time considering the response of second maximum wave height
$FA_4$06$H2$ = The 406-seconds result including response of second maximum wave height

Appendix B

Illustrating the difference between maximum FA-moment and the responses of maximum wave heights

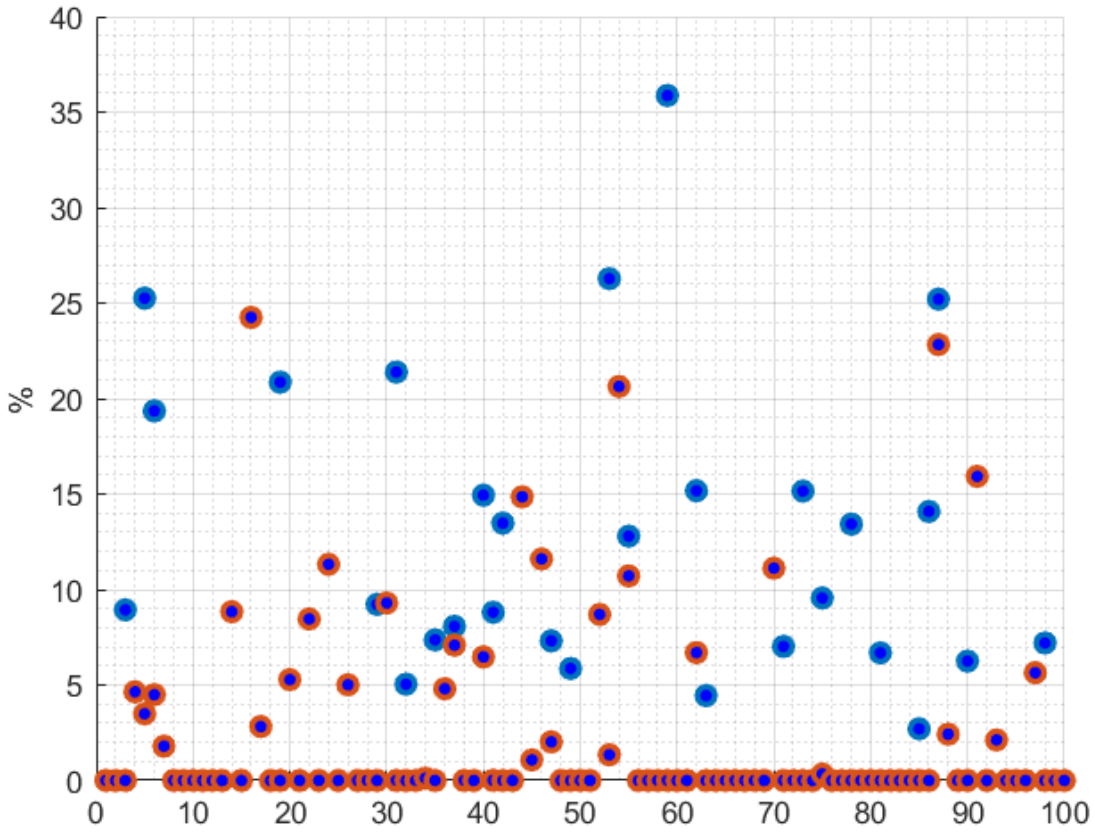

The blue dots are the difference between maximum FA-moment and the response of maximum wave height. The red ones are the difference between maximum FA-moment and the response of two maximum wave hights.Including the one whitch is larger.

Appendix C

The Gumbel probability paper and histogram; Fitting the largest of five maximum response

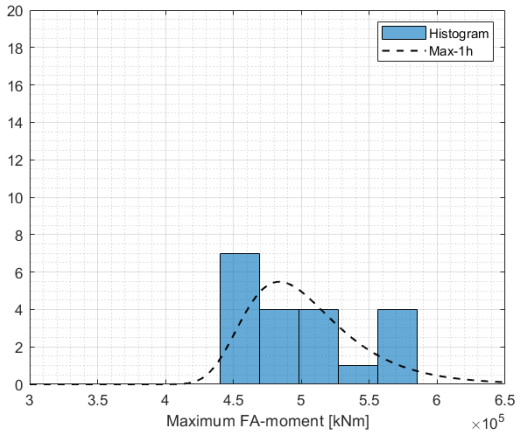

(a) Reference characteristic value

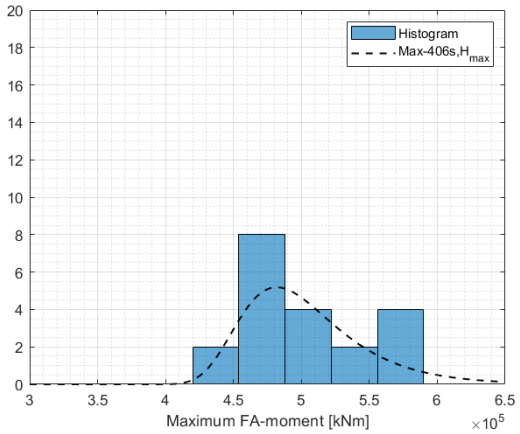

(b) The short simulation approach I

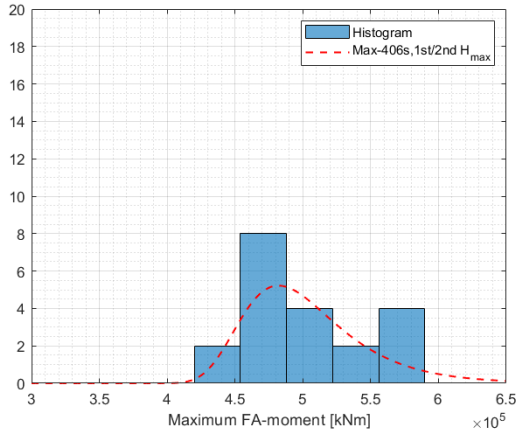

(c) The short simulation approach II

Figure C.1: Histogram vs PDF (fitted Gumbel model)

Reference: the characteristic response generated by 1-hour simulations; maximum of five maximum FA-moment
Approach-I: the characteristic response estimated by short-simulation; approach at maximum wave height;maximum of five
Approach-II: the characteristic response estimated by short-simulation approach, including the response of second maximum wave heigh; maximum of five

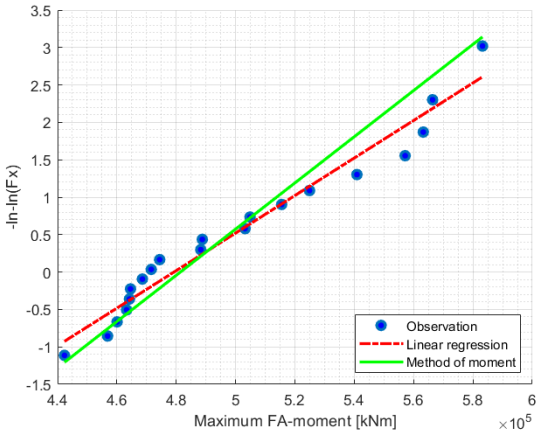

(a) The reference

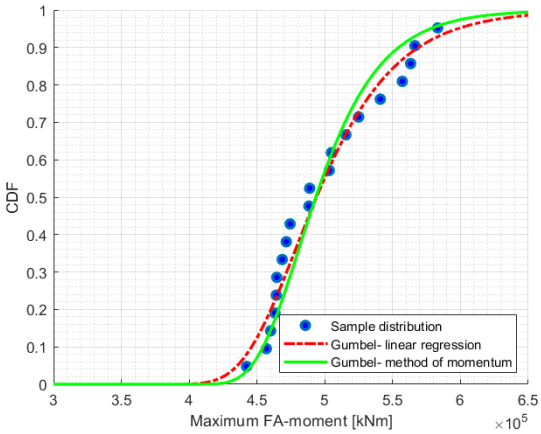

(b) Reference characteristic value

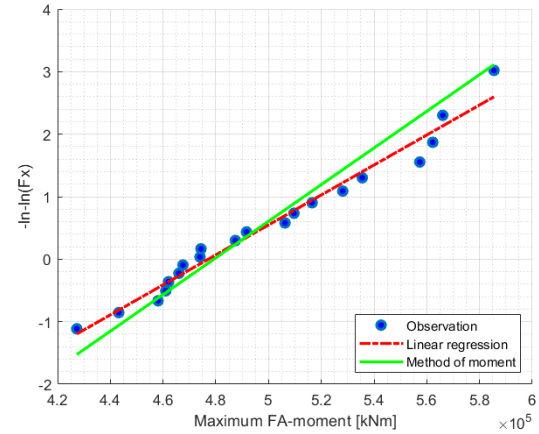

(c) The short simulation approach I

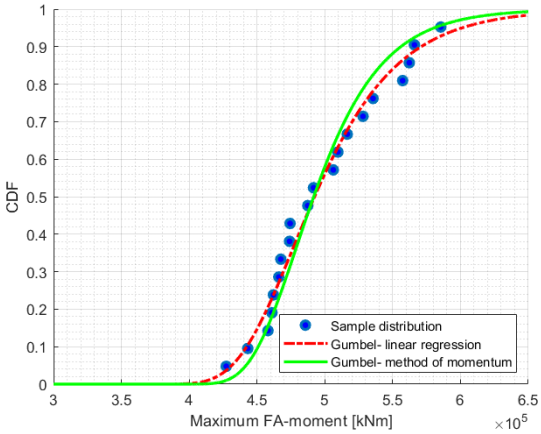

(d) The short simulation approach I

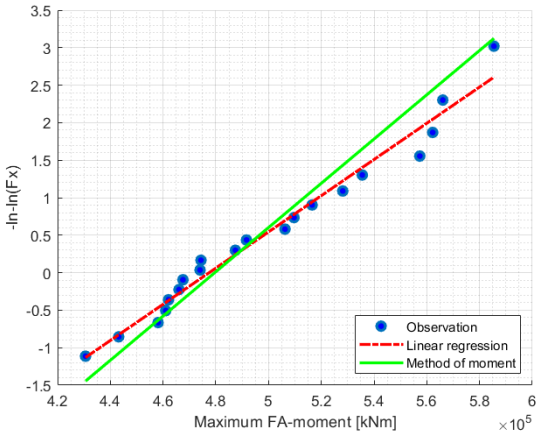

(e) The short simulation approach II

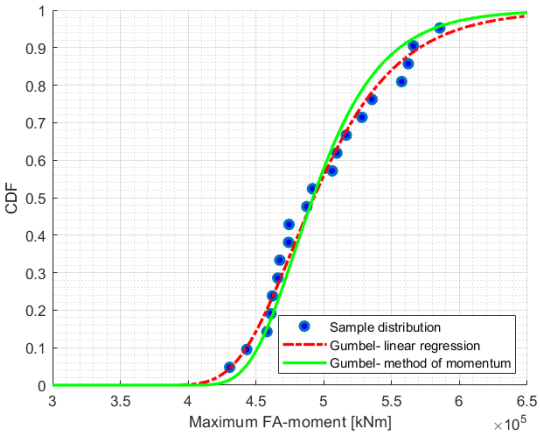

(f) The short simulation approach II

Figure C.2: Testing the fitted gumbel model in probabilty paper

Reference: the characteristic response generated by 1-hour simulations; maximum of five maximum FA-moment
Approach-I: the characteristic response estimated by short-simulation; approach at maximum wave height;maximum of five
Approach-II: the characteristic response estimated by short-simulation approach, including the response of second maximum wave heigh; maximum of five

Appendix D

Simulating realisation of 2.order surface elevation in MATLAB

```
1
2  function waveSimu(simuTime) % input- simulation time in seconds
3                                                  % output 1st, 2nd, 3rd maximum
       height
4
5  %% Parameters;
6  hs=15.6;              % Significiant wave height at site[m]
7  tp=14.5;              % Peak period [s]
8  wp=2*pi/tp;
9  g=9.81;               % gravity accelration [m/s^2]
10 rho=1025;             % sea water dencity[kg/m^3];
11 dw=2*pi/simuTime;     % frequency resolution.
12 w= 0.01:dw:2*pi;      % frequency vector
13 k=w.^2/g;
14 dt=0.2;
15 t=1:dt:simuTime;
16
17 %% JONSWAP
18 gamma= 42.2*((2*pi*hs)/(g*tp^2))^(6/7);       % gamma factor for Joneswap;
19 sigma=0;
20 sw=zeros(1,length(w));
21
22 for i= 1: length(w)
23     if w(i)>wp
24         sigma=0.09;
25     else
26         sigma=0.07;
27     end
28
29     sw(i)=0.0497*(hs^2)*tp*(1-0.287*log(gamma))*(w(i)/wp)^(-5)*exp(-1.25*(w(i)/wp)
       ^(-4)) ...
30         *gamma^exp(-0.5*((w(i)-wp)/(sigma*wp))^2);
31 end
32
33 %% Simulating the linear wave
34 xi=zeros(1,length(t));
35 phi=zeros(1,length(w));
36 xi0=zeros(1,length(w));
37 for j=1:length(w)
38     phi(j)=2*pi*rand;
39     xi0(j)=sqrt(2*sw(j)*dw);
40 end
41
42 for i=1:length(t)
43     for j=1:length(w)
44         xi(i)=xi(i)+xi0(j)*cos(w(j)*t(i)-phi(j));
45     end
46 end
```

```
47
48 %% Simulating the second order terms
49 % The c in the end of variable name means 'cutted'
50 w_lim=sqrt(2*g/hs);      %cutting frequency to calculating the second order terms.
51 wc=w(w<=w_lim);
52
53 beta=zeros(length(wc),length(t));
54 dxi1=zeros;
55 for i=1:length(wc)
56     beta(i,:)=-wc(i).*t+phi(i);
57     dxi1=dxi1+ 0.5*xi0(i)^2*k(i).*cos(2*beta(i,:));
58 end
59
60 dxi2=zeros;
61 dxi3=zeros;
62 for i=1:length(wc)-1
63     for j=i+1:length(wc)
64         dxi2=dxi2+0.5*xi0(j)*xi0(i)*(k(j)+k(i))*cos(beta(j,:)+beta(i,:));
65         dxi3=dxi3-0.5*xi0(j)*xi0(i)*(k(j)-k(i))*cos(beta(j,:)-beta(i,:));
66     end
67 end
68 dxi=dxi1+dxi2+dxi3;
69 xi2=xi+dxi;
70
71 %% presenting the result
72 upCross=1;
73 for i=1:length(t)-1
74     if xi2(i)<=0 && xi2(i+1)>0
75         upCross=[upCross i];
76     end
77 end
78
79 height=zeros(1,length(upCross));
80 for i=1:length(upCross)-1
81    top= max(xi(upCross(i):upCross(i+1)));
82    buttom= min(xi(upCross(i):upCross(i+1)));
83   height(i)=abs(top)+abs(buttom);
84 end
85
86 max1=max(height);
87 max2=max(height(height<max1));
88 max3=max(height(height<max2));
89
90 save('waves','t','xi','xi2')
91
92 end
```

Listing D.1: Surface elevation